universe

MDPI

Article

A Critical Discussion on the H_0 Tension †

Salvatore Capozziello [1,2,3,*], Giuseppe Sarracino [4] and Giulia De Somma [2,4,5]

[1] Dipartimento di Fisica "E. Pancini", Università degli Studi di Napoli "Federico II", Complesso Universitario Monte S. Angelo, Via Cinthia 9 Edificio G, 80126 Napoli, Italy
[2] Istituto Nazionale di Fisica Nucleare (INFN), Sezione di Napoli, Complesso Universitario Monte S. Angelo, Via Cinthia 9 Edificio G, 80126 Napoli, Italy; giulia.desomma@inaf.it
[3] Scuola Superiore Meridionale, Largo San Marcellino 10, 80138 Napoli, Italy
[4] INAF-Osservatorio Astronomico di Capodimonte, Via Moiariello 16, 80131 Napoli, Italy; giuseppe.sarracino@inaf.it
[5] INAF-Osservatorio Astronomico d'Abruzzo, Via Maggini sn, 64100 Teramo, Italy
* Correspondence: capozziello@na.infn.it
† This manuscript is dedicated to the memory of Alexey A. Starobinsky, who recently passed away. He was a distinguished scientist who greatly contributed to the developments of modern cosmology and theories of gravity with his deep insights and outstanding results.

Abstract: A critical discussion on the H_0 Hubble constant tension is presented by considering both early and late-type observations. From recent precise measurements, discrepancies emerge when comparing results for some cosmological quantities obtained at different redshifts. We highlight the most relevant measurements of H_0 and propose potential ideas to solve its tension. These solutions concern the exploration of new physics beyond the ΛCDM model or the evaluation of H_0 by other methods. In particular, we focus on the role of the look-back time.

Keywords: observational cosmology; Hubble tension; look-back time

check for updates

Citation: Capozziello, S.; Sarracino, G.; De Somma, G. A Critical Discussion on the H_0 Tension. *Universe* **2024**, *10*, 140. https://doi.org/10.3390/universe10030140

Academic Editors: Galina L. Klimchitskaya, Vladimir M. Mostepanenko and Sergey V. Sushkov

Received: 27 January 2024
Revised: 8 March 2024
Accepted: 10 March 2024
Published: 13 March 2024

Copyright: © 2024 by the authors. Licensee MDPI, Basel, Switzerland. This article is an open access article distributed under the terms and conditions of the Creative Commons Attribution (CC BY) license (https://creativecommons.org/licenses/by/4.0/).

1. Introduction

The Λ Cold Dark Matter (ΛCDM) model is considered the cosmological standard, capable of describing the observed Universe by fixing only six free parameters [1]. These are the dark matter density, the baryon density, the observed angular size of the sound horizon at recombination, the scalar spectral index, the curvature fluctuation amplitude, and the reionization optical depth.

Applying general assumptions on these parameters, it is possible to derive the other cosmological quantities, including the Hubble constant H_0 and the other cosmographic parameters [2]. The result is a self-consistent picture of our Universe in good agreement with observations.

This relatively simple model is able to describe a large part of the history of the Universe with good precision, from the end of the so-called inflationary era [3,4] to the current epoch. According to the ΛCDM, our Universe is composed by three major constituents: a cosmological constant Λ, associated with the so-called dark energy, accounting for approximately 68% of the total density, a cold (non-relativistic) dark matter component, which should account for 27% of the cosmic pie [1,5–17], and lastly, the remaining 5%, composed by baryonic matter, stars, galaxies, and all the luminous structures. The accuracy of this model is remarkable when compared with cosmological observations, such as the accelerated expansion of the Universe [7] deduced from the observed light curves of Supernovae Type Ia (SNe Ia). Cosmic acceleration can be addressed by the presence of a cosmological constant or, in general, by some unknown form of dark energy, acting as a negative pressure in the cosmological equations.

On the other hand, dark matter was initially introduced to account for the virial theorem applied to clusters of galaxies [18]. Subsequent observations revealed that it is

also a fundamental component needed to explain the rotation curves of galaxies, which, otherwise, would not be well fitted by Newtonian dynamics [19,20] if only galactic baryonic components are taken into account.

Despite its overwhelming successes, the ΛCDM model presents some critical issues that captured the attention of scientific community. The most relevant challenges are the nature of dark energy and dark matter, as well as the ongoing tension of the Hubble constant derived by different measurements at different scales. After decades of precise measurements and tests [17,21–23], no direct or indirect evidence of exotic particles constituting cosmic dark fluids has been found. Consequently, according to the ΛCDM model, we have no final answer, at the fundamental level, on the constituents of the observed Universe for approximately 95%.

A further issue is related to the H_0 tension, that is the discrepancy between the late-type measurements of H_0 [24], usually linked to the cosmological ladder [25,26] , and the early-type ones, associated with measurements of the Cosmic Microwave Background Radiation (CMBR). The most recent results from two prominent collaborations, SH0ES and Planck, report values of H_0 as 73.04 ± 1.04 km/(s Mpc) at a 68% confidence level (CL) for the former [24] and 67.4 ± 0.5 km/(s Mpc) at 68% CL for the latter [1]. As it stands, there is a 5σ tension between these two measurements [24], which, in principle, should provide the same result. Furthermore, this tension extends beyond these two collaborations and involves several late and early-type observations [25].

To address these issues, different approaches have been considered like extensions of General Relativity (GR), on which the ΛCDM model is based. For instance, a particular extension, known as $f(R)$ gravity [27–32]), has been considered in cosmological applications [33–37] to address different issues related to the ΛCDM model, like the late-time dark energy [14,27], and the early inflationary behavior [4]. The philosophy of these approaches is that, instead of searching for new exotic ingredients, the gravitational sector should be improved according to the scales. In this perspective, the H_0 tension could also be fixed improving geometry [29,38–40].

Other alternatives imply Extended Theories of Electromagnetism or the improvement of the Standard Model of Particles [41–43]. Furthermore, the H_0 tension could be also related to some fundamental quantum concepts, like the Compton Length and the Heisenberg Uncertainty Principle, applied to the cosmological setting [44,45].

Finally, under the standard of "new physics" a large amount of investigations have been pursued both in early and late Universe [46–74].

A recent research line explores the possibility of a "variable H_0 constant", i.e., the idea that the measured value of the Hubble constant might depend on the redshift (i.e., the scale) at which it is measured [75–89]. In this context, the H_0 constant can be evaluated by the look-back time [90]. The approach consists in determining H_0 at any redshift z starting from the look-back time of the related sources.

In this paper, a critical discussion on H_0 tension will be presented. The outline is the following. Section 2 provides a brief summary of the ΛCDM model. Section 3 is devoted to the most prominent measurements related to H_0. In Section 4, we discuss the look-back time approach to the H_0 tension starting from the results in [90]. Section 5, a redshift-dependent H_0 is considered. We explore, in particular, its consequences on cosmological distances. In Section 6, we discuss the results and draw conclusions.

2. A Summary of the ΛCDM Model

The ΛCDM model is a straightforward byproduct of GR. Assuming the Cosmological Principle, the Universe is homogeneous and isotropic beyond a certain scale, which is, more or less, over ∼120 Mpc. This assumption is supported by several observations considering large sets of data [25,91–93]. The Cosmological Principle is implemented by the Friedman-Lemaître-Robertson-Walker (FLRW) metric [94]:

$$ds^2 = c^2 dt^2 - a^2(t)\left[\frac{dr^2}{1-kr^2} + r^2\Omega^2\right], \tag{1}$$

where Ω represents the angular component of the metric, $a(t)$ is the scale factor, and k is the spatial curvature constant. It can be equal to $-1, 0, 1$ depending on the curvature of the cosmological spatial submanifold. According to Equation (1), the Einstein field equations can be recast as:

$$\left(\frac{\dot{a}}{a}\right)^2 + \frac{kc^2}{a^2} = \frac{8\pi G\rho}{3} + \frac{\Lambda c^2}{3}, \tag{2}$$

$$\frac{\ddot{a}}{a} = -\frac{4\pi G}{3}\left(\rho + \frac{3p}{c^2}\right) + \frac{\Lambda c^2}{3}, \tag{3}$$

which are the Friedman equations leading the cosmological expansion [95]. These equations are complemented by the continuity equation and the equation of state defined as:

$$\dot{\rho} + 3\frac{\dot{a}}{a}\left(\rho + \frac{p}{c^2}\right) = 0 \tag{4}$$

$$p = w\rho c^2. \tag{5}$$

Here, G is the gravitational constant, p is the pressure, ρ the density, w is the cosmological equation of state parameter, equal to -1 for the ΛCDM model, and Λ is the cosmological constant. These are the equations on which dynamics of ΛCDM model is based. The scale factor can be written as a function of the redshift as follows [2]:

$$a(t) = \frac{a_0}{(1+z)}, \tag{6}$$

where $a_0 = 1$ is the scale factor normalized at our epoch. This allows us to write the cosmological distances as a function of the redshift [96]. It is possible to rewrite Equation (2) in terms of the cosmological densities as follows [97]

$$\frac{H^2(z)}{H_0^2} = \Omega_r(1+z)^4 + \Omega_M(1+z)^3 + \Omega_k(1+z)^2 + \Omega_\Lambda, \tag{7}$$

where $H(z) = \dot{a}/a$ is the Hubble Parameter, H_0 is the Hubble Constant, i.e., the Hubble parameter derived for $z = 0$, thus for the Universe at our epoch, Ω_R is the radiation energy density parameter, Ω_M is the matter density parameter, where both dark and luminous matter are taken into account, Ω_k is the "density" associated to the curvature, being equal to zero for a flat Universe, and Ω_Λ is the density associated with the cosmological constant. All these quantities, apart from $H(z)$, are derived at present epoch. From this equation, we can define

$$E(z) = \frac{H(z)}{H_0} = \sqrt{\Omega_r(1+z)^4 + \Omega_M(1+z)^3 + \Omega_k(1+z)^2 + \Omega_\Lambda}. \tag{8}$$

This equation allows us to express cosmological distances as a function of $E(z)$. It is worth noticing that $E(z)$ depends only on the redshift and the densities of the today Universe, while it does not depend directly on H_0. The luminosity distance $d_L(z)$, derived from the intrinsic luminosity and the photon flux received by a given cosmological source, is:

$$d_L(z) = (1+z)d_M(z)\,, \tag{9}$$

where $d_M(z)$ is the transverse comoving distance. It is

$$d_M(z) = \frac{c}{H_0}\int_0^z \frac{dz'}{E(z')}, \tag{10}$$

for a flat Universe with $\Omega_K = 0$.

For an open Universe with $\Omega_K > 0$, it is

$$d_M(z) = \frac{c}{H_0\sqrt{\Omega_K}} \sinh\left(\frac{H_0\sqrt{\Omega_K}}{c}\int_0^z \frac{dz'}{E(z')}\right). \tag{11}$$

For a closed Universe with $\Omega_K < 0$, it is

$$d_M(z) = \frac{c}{H_0\sqrt{|\Omega_K|}} \sin\left(\frac{H_0\sqrt{|\Omega_K|}}{c}\int_0^z \frac{dz'}{E(z')}\right). \tag{12}$$

The luminosity distance is essential in observational cosmology because it can be associated with the "standard candles". These are astrophysical objects whose intrinsic luminosity can be derived from some intrinsic physical mechanism. Such a mechanism is generally correlated with quantities that are independent of the source distance, and so can be used to measure $d_L(z)$ intrinsically. Standard candles are a key component of the cosmic distance ladder and play a crucial role in determining H_0.

Another important tool for the estimation of cosmic distance ladder is the angular diameter distance, defined as

$$d_A(z) = \frac{d_M(z)}{(1+z)}. \tag{13}$$

It is important because it is linked to the "standard rulers" (i.e., astrophysical objects whose geometrical features can be deduced from their intrinsic physics). We will describe a particular probe employing this definition. Finally, another very important distance definition is linked to the look-back time, which is the time the photon takes to reach us from a certain redshift. It is defined as:

$$T_{lt}(z) = \frac{1}{H_0}\int_0^z \frac{dz'}{(1+z')E(z')}. \tag{14}$$

It is strictly connected to the light-travel distance, i.e., the path traveled by the photon to reach us from an astrophysical source in the expanding Universe. It is

$$d_{lt}(z) = cT_{lt}(z). \tag{15}$$

The last two equations are the starting point for the analysis presented in [90], and the novel discussions presented in this work. We have to note here that, in all the cosmological distance definitions, H_0 plays the role of a normalization constant, as it is not directly involved in the integral functions, which, in turn, depend only on the different cosmological components and the redshift.

3. The H_0 Measurements and the Tension

Over the past decades, several methods and astrophysical sources have been employed to measure H_0 with high precision allowing us to obtain, remarkably, very small uncertainties on the measurements [17,25]. This new era of precision cosmology is also the main reason for the H_0 tension, which is at the center of attention of the scientific community. As previously mentioned, we observe a significant 5σ tension between the latest SH0ES and Planck collaborations' results [1,24], but, as we will see, these derivations are actually representative of two entire sets of measurements: the former of the early-type and model-dependent observations, while the latter of the direct late-type and model-independent ones.

3.1. Late and Early-Type Measurements

Regarding the late-type measurements, many observations, including those by the SH0ES collaboration, are based on the cosmic distance ladder method. In this approach, each step builds upon the previous one through calibration methods, especially in redshift regions where multiple probes are available. This method enables us to reach relatively

deep redshift ranges while preserving the precision provided by low-redshift probes, renowned for their accuracy.

The cosmic distance ladder consists of three primary steps [24,98]. The first involves precise geometric distance measurements, allowing us to directly calculate the distances of nearby objects. This step is reliable because depends on a straightforward geometrical method and does not require extensive knowledge of the astrophysical probe used for distance measurement. There are three possible anchors for this first rung: Milky Way Cepheid parallaxes, detached-eclipsing binary measurements in the Large Magellanic Cloud [99], and the water-maser host NGC 4258 [100,101]. These three anchors provide approximately 1%, 1.2%, and 1.5% precision in the calibration of H_0, respectively. In recent years, a strong improvement in the Cepheid parallax measurements has been provided by the European Space Agency (ESA) Gaia mission [102–105]. Gaia, designed for astrometry, photometry, and spectroscopy, has created the most accurate 3D map of the Milky Way. The latest release, covering the first 34 months of observations, has provided the largest dataset of Cepheids ever (around 3000 Milky Way Cepheids) allowing us to measure the parallaxes and consequently the distances of Cepheids with unprecedented accuracy [106].

The second step involves primary distance indicators, often Classical Cepheids, which exhibit an intrinsic relationship between their luminosities and periods, the so-called Period-luminosity relation (PL) [107–109]. Although this step is valuable, it may be influenced by potential systematic effects such as the metallicity dependence of the coefficients of the PL relation, which need to be addressed [110–113].

The third step includes probes like SNe Ia, which use primary distance indicators as anchors in regions where both are detected. SNe Ia, with their higher luminosities, can explore relatively high-redshift regions.

Let us discuss in more detail how the SNe Ia are employed as standard candles, given that they are one of the most important components of the cosmological ladder approach [114]. The most updated SNe Ia dataset is the Pantheon+ sample [115], which was used for the latest H_0 measurements [24,116] and serves as a natural successor to the earlier Pantheon set. [117]. The Pantheon+ sample is composed of 1701 lightcurves taken from 1550 different SNe Ia, covering a redshift range from $z = 0.01$ up to $z = 2.26$.

In general, the physics behind these astrophysical objects is well-understood. SNe Ia are the byproduct of the explosions of white dwarfs in binary systems exceeding the Chandrasekhar limit due to mass transfer from their companion star. Since this limit is a fundamental constraint for the stability of all white dwarfs, all SNe Ia light curves share similar features. Specifically, the prevailing model, consistent with the majority of SNe Ia observations, is the single-degenerate Chandrasekhar mass explosion [118]. In this model, the white dwarf accretes mass from its less evolved companion star, typically a red giant, which has a significantly lower density, especially in its outer regions. SNe Ia light curves are well-fitted by the deflagration model shown in [119]. They are primarily powered by the β-decay of the radioactive isotope ^{56}Ni produced during the explosion [120].

Observationally, this model predicts that SNe Ia light curves typically exhibit an absolute magnitude around $\mathrm{M} \simeq -19$ [121]. However, both super-luminous [122] and sub-luminous [123] SNe Ia have been observed, suggesting the involvement of more complex mechanisms, such as the delayed detonation scenario for super-luminous SNe Ia [124]. Even so, a phenomenological relation has been observed between the peak magnitude of the light curve and the luminosity decline rate in each SN Ia [125], which makes them a proper standardizable candle. Their use as a cosmological probe is based on the following equation

$$\mu_{th,SNeIa} = m - M = 5\log(d_L) + 25, \tag{16}$$

where m is the apparent magnitude of the astrophysical object, M is its absolute magnitude, and the luminosity distance is expressed in Mpc. This quantity is confronted with the detected distance modulus μ_{obs} of the SNe Ia, from which a best-fit of the desired cosmological parameter (as well as of the absolute magnitude M) can be performed by employing the following χ-squared function

$$\chi^2_{SNeIa} = (\mu_{th} - \mu_{obs})^T \times \mathcal{C}^{-1}_{SNeIa} \times (\mu_{th} - \mu_{obs}) \,, \tag{17}$$

where $\mathcal{C}^{-1}_{SNeIa}$ is the inverse of the covariance matrix [81].

It is worth noticing that the absolute magnitude of SNe Ia is treated as a general parameter. This introduces a degeneracy with H_0, which can be resolved either by fixing M to a certain value or through calibration processes involving primary distance indicators like Classical Cepheids in the cosmological ladder approach [115].

Furthermore, alternative probes can be employed in the cosmological ladder approach. For instance, the tip of the red giant branch (TRGB) [126], in place of the Classical Cepheids [127], or type II SNe [128], the Tully-Fisher relation for galaxies [129], and surface brightness fluctuations [130], as substitutes for SNe Ia in the corresponding cosmological step. The surface brightness fluctuations have also been used as primary distance indicators [131]).

Regarding the results obtained from these methods, a general consensus has emerged around the values derived by the SH0ES collaboration. Indeed, their data have been reanalyzed using different statistical methods, without a significant modification of the final results [25,132–137]. Some investigations have also included Cepheids from outside our Galaxy, to address potential biases in measurements linked to specific Cepheid populations [101].

An alternative calibration of the SNe Ia, using the TRGB methodology, has produced results that differ from those provided by the SH0ES Collaboration. For example, studies by [127,138,139] derived a value of $H_0 = 69.6 \pm 1.9$ km/(s Mpc) at a 68% confidence level, which falls between the values from SH0ES and Planck collaborations. However, there are other studies involving the use of TRGB as calibrators for SNe Ia whose results are consistent with the other late-type observations [140–144]. This has led to ongoing discussions about TRGB-based observations [131,145], particularly regarding methodologies to account for potential systematic effects [138,141] and a possible empirical relation between different TRGB observations, similar to what has been derived for Classical Cepheids [145].

As mentioned earlier, the cosmological ladder can be used by considering also other probes, such as the surface brightness fluctuations of galaxies, as alternatives to the SNe Ia, or as an intermediate step between Cepheids and SNe Ia [146]. The results remain consistent with the other late-type measurements, even if there are higher errors in the determinations of H_0 from these sources [130,147]. A similar approach can also be employed for SNe type II [128,148], and the Tully-Fisher relation for galaxies [129,149,150], obtaining results which remain consistent with the SH0ES collaboration.

While the cosmological ladder is an intuitive method for determining H_0 independently from the cosmological model, it requires very precise knowledge of the astrophysical processes associated with each used probe, especially in the first steps of the ladder. This is because any potential unaccounted-for systematic effect in the first rung could propagate to subsequent ones, as they are calibrated on the preceding. Therefore, using alternating astrophysical objects for the same step becomes a crucial test, as the cross-test between different collaborations using the same probes, to identify and remove possible systematic issues.

The cosmological ladder framework is not the only possible methodology for estimating H_0 at late times. An example is the strong lensing time delay estimates, which are independent of cosmological models but do require assumptions about foreground and lens mass distributions [25]. Even with this independent alternative method, the results remain consistent with the other late-type approaches [151–154]. It is interesting to mention that, in [154], a decreasing trend in the measure of H_0 with the redshift has been noted, in agreement with the previously mentioned "variable H_0 constant" [75,81,90,155], which will be the focus of the following analysis.

As we can see, for the late-type measurements, different probes and different methods provide results that are generally in agreement (apart from some exceptions). We may conclude that the tension is very unlikely to be due to systematic or statistical problems in the data themselves, but rather due to a more intrinsic, physical issue. Indeed, different

averages of the late Universe estimates of H_0 are in a 4.5–6.3σ tension with values provided by the Planck Collaboration [25,156,157].

Let us now discuss measurements of H_0 based on assumptions and observations related to the early physics of the Universe. In addition to the latest values derived by the Planck Collaboration [1], there are other independent measurements, involving CMBR, all of which consistently yield lower values for H_0 if compared to late-type observations [158–160].

Early-time phenomenology can be traced even at low redshift values, with notable examples derived through various probes including the Baryon Acoustic Oscillations (BAO) [161–165], Big Bang Nucleosynthesis measurements of the primordial deuterium [166], and weak lensing measurements [16]. These probes yield H_0 estimates consistent with those of Planck Collaboration [165], and different data reanalyses support these results [73,74,167–173]. However, it is essential remembering that early-type measurements are model-dependent, and work within the ΛCDM scenario and the Standard Model. Without these assumptions, constraints on H_0 and other cosmological parameters are remarkably loosened [25,174]. Additionally, these measurements provide estimates for all the six free parameters underlying the ΛCDM model, which, in turn, are used to derive all the other cosmological parameters from the observation of the CMBR peaks.

Let us go into more detail about the BAO. They are also utilized independently for cosmological computations [165] because they consider another kind of cosmological distance, the angular-diameter one. BAO are widely used in literature to complement various analyses with other probes, see Refs. [42,175], and in standalone cosmological computations [165].

BAO are density fluctuations of the visible baryonic matter, caused by acoustic density waves in the early primordial plasma. As such, they are relics of phenomena occurred in early times and observed at lower redshift values such as in cluster formations and galaxy distributions. These phenomena are closely related to the acoustic peaks measured from the CMBR [161] which result from cosmological perturbations generating sound waves in the relativistic plasma of the early Universe [176].

In the past decade, BAO-related measurements have significantly improved in precision [165], which has proven to be mandatory for modern cosmological applications. This is because the acoustic features in matter correlations are relatively weak and occur at large scales [161,177].

Furthermore, these acoustic peaks are associated with different behavior of ordinary and dark matter when they are solicited by perturbations. Ordinary matter expands as a spherical wave, while dark matter remains in place [178]. After this event, both dark matter and baryon perturbation start the formation of large-scale structures. Given that, the central perturbation in the dark matter dominates over the baryonic shell, the acoustic feature is manifested as a single spike in the correlation function at approximately 150 Mpc between pairs of galaxies. This scale is typically close to the sound horizon [179].

It is important to note that, given their nature, behind each BAO-related measurement, there are tens of thousands of observations regarding large structures such as galaxies or clusters of galaxies. The largest spectroscopic survey to date is the Baryon Oscillation Spectroscopic Survey (BOSS [180]), one of the main objectives of the Sloan Digital Sky Survey (SDSS)-III Collaboration [181]. Indeed, this collaboration conducted spectroscopy on over 1.5 million galaxies, generating valuable BAO-related data points. This dataset was later complemented by the extended Baryon Oscillation Spectroscopic Survey (eBOSS [182]), which was the cosmological survey within the SDSS-IV [183].

As previously stated, BAO may be used as cosmological probes starting from the angular-diameter distance. However, unlike SNe Ia, BAO-related measurements can vary in their definitions. For instance, in the set composed of 16 BAO employed in [42,43,175], compiled from [162–165,184], some of the data offer information about the following quantity

$$d_V(z) = \left[{d_M}^2(z) \frac{cz}{H(z)} \right]^{\frac{1}{3}}, \tag{18}$$

where d_M is the transverse comoving distance defined in Equations (10)–(12) and $H(z)$ is defined in Equation (7). Also, other cosmological quantities inferred by BAO are the following parameter

$$A(z) = \frac{100 d_V(z)\sqrt{\Omega_M h^2}}{cz}, \tag{19}$$

where $h = H_0/(100 \text{ km s}^{-1} \text{ Mpc}^{-1})$; the so-called Hubble distance

$$d_H(z) = \frac{c}{H(z)}, \tag{20}$$

and the comoving distance itself. It is important to emphasize that all these definitions are interconnected, but they are not identical. This is a relevant point when constructing the covariance matrix using these heterogeneous measurements.

Additionally, it is worth noting that the majority of the BAO measurements have been rescaled by a factor denoted as r_d, that is the distance between the end of inflation and the decoupling of baryons from photons after the recombination epoch. The value of this factor is approximately 150 Mpc and it is defined as [165].

$$r_d = \int_{z_d}^{\infty} \frac{c_s(z)}{H(z)} dz, \tag{21}$$

where $c_s(z)$ is the sound speed, while z_d is the redshift of the drag epoch, which in turn corresponds to the time when baryons decouple from the photons. This decoupling typically occurs at a redshift of $z \approx 1020$, a value influenced by the physics of the early Universe. This quantity can be approximated using a formula involving cosmological parameters [185], that is

$$r_d = \frac{55.154 \cdot e^{[-72.3(\Omega_\nu h^2 + 0.0006)^2]}}{(\Omega_M h^2)^{0.25351} (\Omega_b h^2)^{0.12807}} Mpc, \tag{22}$$

where Ω_b is the baryonic density and Ω_ν is the neutrino density. It is important to notice that, although they are observed in lower redshift regions, their link to early-Universe physics implies that the cosmological computations derived from them are consistent with the Planck Collaboration results, including those related to H_0 [165].

3.2. Overcoming the Tension

The H_0 tension is one of the most compelling problems of modern cosmology, and, as such, both observational and theoretical approaches have been explored by the scientific community to address it. From the former point of view, a new independent window has opened by the observations of gravitational waves [186]. Indeed, these detections have already been used as 'standard sirens', to derive new estimates for H_0 [187–190].

At present, the precision of these measurements does not allow us to understand if they reduce the tension or if they are more in agreement with either the early or late-type measurements. However, given that we are still in the early stages of the gravitational waves era, a considerable improvement is expected from future observations, especially from the next generations of gravitational wave detectors. This holds great potential as a completely independent, non-electromagnetic method for measuring H_0, providing a new window to solve the tension issue.

Other important measurable quantities for the cosmological studies are the look-back time and the related age of the Universe, which have been used to infer H_0 observationally, as it is the case of the ages of the observed astrophysical objects [155,191–195].

Furthermore, interesting observations of high redshift galaxies have been performed by the James Webb Space Telescope. The observed galaxies appear to have unexpectedly high stellar masses which may be in conflict with the age of the Universe as inferred by

Planck [196]. It remains unclear whether this potential discrepancy may be attributed to galaxy evolution models or if it has a cosmological origin.

Another possible independent method to infer H_0 is based on the $H(z)$ function and its evolution with the redshift, allowing us to extrapolate H_0 by requiring $z = 0$. This would be a completely model-independent procedure being able to derive this value, independently from other methodologies. A possible approach for this analysis is based on the so-called cosmic chronometers [26,197], i.e., the age evolution of galaxies, as well as on techniques like Gaussian Process regression [198,199], or cosmography via different polynomials [14,36,200]. These approaches have provided estimates of H_0 ranging from values consistent with Planck collaboration to values consistent with late-type estimates [25]. It is important to note that an extrapolation of H_0 at $z = 0$ from the $H(z)$ function could be in contrast with assuming a variable H_0. We will discuss this point in the next section.

From an observational standpoint, another potential approach to address the H_0 tension involves the extension of cosmological ladder to higher redshift, in view to bridge the gap between early and late-type measurements. For this aim, one needs to observe astrophysical objects at high z acting as standard candles. An example is represented by the Gamma-Ray Bursts (GRBs), for which different correlations between their intrinsic physical parameters can be observed [201–205], allowing us to use them as distance indicators [71,72,175,206–211].

Other promising high-redshift indicators are Quasars [212]. For these objects, empirical correlations among physical parameters have been found, so, as in the case of GRBs, they could constitute a formidable and populated set of objects to test the Universe at high redshift [213–218].

From a more theoretical point of view, the idea that new physics could be behind the tension is fascinating the scientific community, especially if one considers that this is not the only issue that the ΛCDM model, and more in general GR itself, presents [17,29]. Other notable examples are the nature of dark energy and dark matter that seems to escape any probe at fundamental level. A popular approach to address these issues is to consider extensions of ΛCDM model and GR. As previously mentioned, $f(R)$ gravity [29] and other modified theories [17,39] have been applied for various cosmological and astrophysical tests [17,39,82,84,85,219,220].

These modifications include the possibility of treating the dark energy component as a variable fluid rather than a cosmological constant [221,222]. This constant can be represented by a scalar field ϕ rolling slowly down a flat component of a potential $V(\phi)$ and giving rise to the models known as quintessence [223]. In this sense, the Chevallier-Polanski-Linder (CPL) parameterization for the dark energy component [224,225] is one of the most widely studied modifications to the standard scenario.

Other possible approaches include models where interactions between dark energy and dark matter are taken into account [226,227]. The main issue of this framework is the degeneracy existing between different models, which try to address the same problems in completely different ways, thus not allowing us to achieve a natural and definitive extension of the ΛCDM model and GR [228–230].

New physics may also be linked to modifications of the underlying phenomenology at both the early and late stages of the Universe [25,88]. Examples for early epochs include:

1. Early Dark Energy, which behaves as a cosmological constant for $z \leq 3000$, and then decades as fast as the radiation density (or even faster) at late times [50,52,231] via a slow-roll phase transition. While promising, this approach presents problems from both observational and theoretical perspectives [232]. Therefore, a modification has been proposed, called New Early Dark Energy, where instead of a slow phase transition, we have an almost instantaneous one [233]. This idea is similar to the aforementioned quintessence for late times.
2. Extra relativistic degrees of freedom at the recombination, parameterized by the number of neutrino species, N_{eff}. According to our current understanding, for active

massless neutrino families $N_{eff} \sim 3.044$ [234]. This number affects the inferred value of H_0. Various models regarding further dark radiation have been proposed [235–238].

3. Modifying the recombination history, by shifting the sound horizon for BAO at recombination. This can be achieved by either varying the early-time expansion history or by modifying the redshift of recombination. Various methods have been proposed to accomplish this, including exotic scenarios in the early Universe [239–241].

The proposed new physics at late times modifies our interpretation of dark energy in various ways. Apart from what we have mentioned before, we recall the following:

1. Considering a cosmological bulk viscous fluid, characterized by a peculiar form of its pressure term, which is made up of two parts, where the first one is the usual component linked to the density via an equation of state, while the second is linked to the viscosity [242–245].
2. A chameleon field for dark energy, whose mass varies in accordance with the matter density of the considered environment, and whose variability would imply a measurement on H_0 dependent on the particular region in which has been performed [246–250].
3. Diffusion models, implying an interaction between dark energy and dark matter via a non-conserved energy tensor $T_{\mu\nu}$ [251–253], which seems to reduce the H_0 tension with different types of matter fields [254].
4. General dynamical behavior for dark energy, following a philosophy similar to the CPL parameterization. In this sense, one could define emergent dark energy, which has had no effects in the early stages of the Universe, as it completely emerges at late times [255–257].
5. A Running Vacuum model, linked to possibly Quantum Field Theory or String Theory, could be used to explain theoretically a possible phenomenological dependence of cosmological and gravitational constants with the cosmic time [258,259]. This kind of model can actually encompass different assumptions regarding the behavior of dark energy. It has also been successfully tested [260,261].
6. The presence of local inhomogeneities that could affect the late-time measurements of H_0, which may be either due to possible observational issues like incomplete sky sampling, astrophysical problems like incorrect modelling of the local structures, or a more fundamental nature, like the departure of the FLRW assumption at very small scales [262–266].

Alternatives to extensions of GR have also been sought. These alternatives include considerations for potential extensions of the Maxwellian Electromagnetism [267] in a cosmological setting, introducing a second, optical component to the measured redshift of astrophysical sources in cosmological models without dark energy [41–43].

In order to represent a valid alternative to the ΛCDM model, evidence of this kind of effect has to be found. A possible approach is to investigate the upper limits on the photon mass [268–271], especially considering that some extensions propose massive photons [272,273].

Another investigated possibility is dealing with the H_0 tension as an evidence of a more fundamental limit on observations, linked to Quantum Mechanical concepts like the Compton Length and the Heisenberg Uncertainty Principle [44,45]. This approach seeks for addressing the tension without attributing it to unlikely experimental errors or unknown novel physics.

The previously mentioned alternatives offer promising solutions for addressing the H_0 tension and providing a satisfactory explanation for its existence. The main issue is to determine if one of these alternatives truly resolves the tension or if the solution lies within a completely different framework. To accomplish this issue, one not only needs to provide definitive evidence of peculiar effects beyond the ΛCDM model, but also to build up an appropriate extension of the standard framework containing not only novel ideas to solve the H_0 and other tensions but also retaining the outstanding success achieved by GR and ΛCDM model when they are compared with observations.

As said, a novel approach considers the possibility of an evolution of H_0 constant with redshift as a way to address the tension [75–88]. In this sense, the evolution of H_0 and the corresponding tension are considered as a sort of "diagnostics" of a symptom of the breaking-down of the ΛCDM model (or even of the FLRW metric, because it would suggest, according to this interpretation, that the parameterization $H(z) = H_0 E(z)$ is not working), marking the points in which observations are not consistent with the model [75–80].

In this context, a dependence of H_0 on the redshift has been observed in real SNe Ia data and interpreted through the $f(R)$ gravity formalism [81–85,88]. More specifically, in [81], a functional form

$$H_0^z = H_0/(1+z)^\alpha, \tag{23}$$

has been assumed and fitted with the Pantheon set of SNe Ia [117]. Results show that α is not consistent with 0 within 1σ, hinting at a smooth, slow, but continuous, decrease in H_0 value with the redshift. A variable H_0 could be due to a possible break-down, at some scale, of the Cosmological Principle on which the ΛCDM model is based (for general reviews, see [25,229,274], for discussions on diagnostics, see [77,155,264,275]).

It is worth emphasizing that H_0 measurements discussed in this section represent only a part of those obtained in recent years. For a more comprehensive overview, refer to Figure 1 taken from [25].

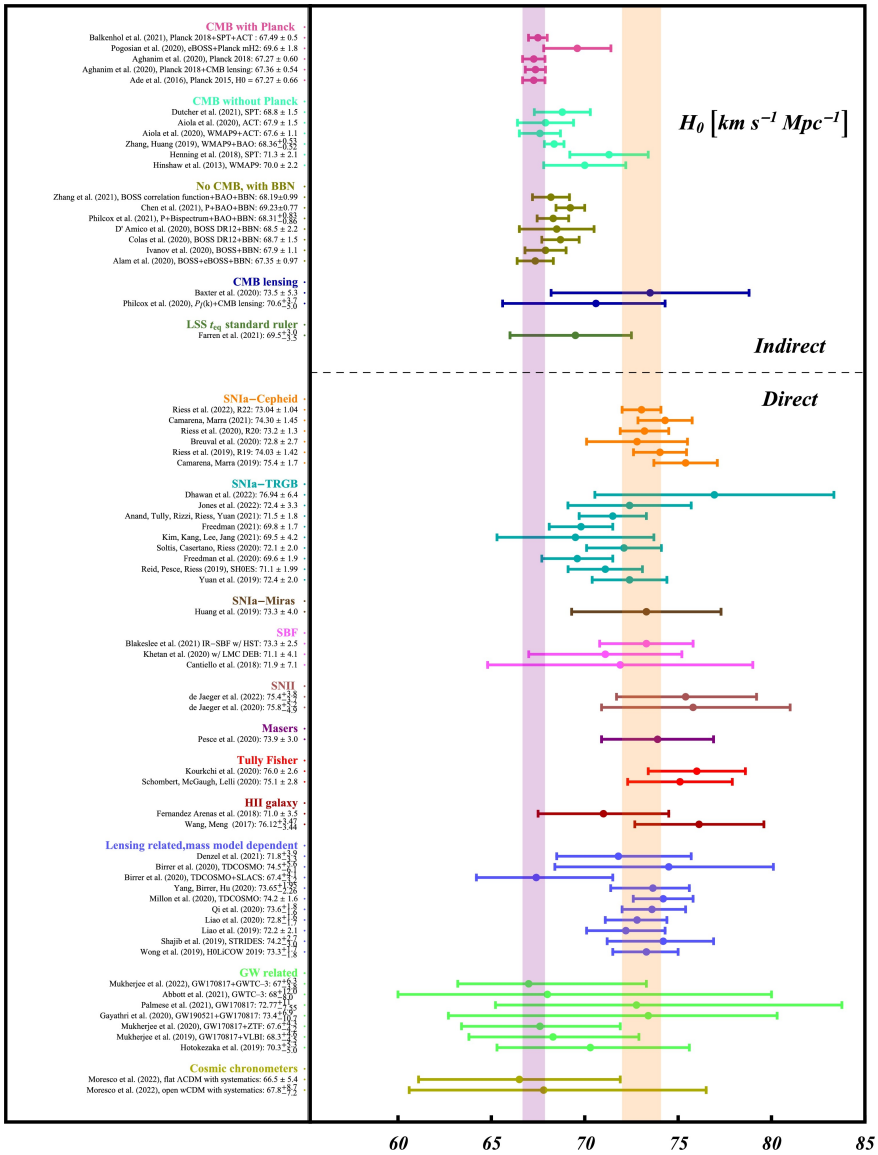

Figure 1. A summary of H_0 measurements performed both at early and late times. Credits to [25].

4. The H_0 Tension and the Look-Back Time

4.1. The $T(z)$ Parameterization

Let us now delve into the approach proposed in [90], where H_0 is derived from the look-back time defined in Equation (14). We will further discuss and improve this parameterization. Let us start from showing that, operatively, we can take into account a Taylor expansion of the scale factor as follows

$$a(t) = a_0 + \frac{d(a(t_0)}{dt}[T(z) - T_0] + \ldots = a_0 + H_0[T(z) - T_0] + \ldots . \tag{24}$$

We can assume that $a_0 = 1$ and approximate $H_0 = 1/T_0$, where T_0 is the age of the Universe today. This approximation is at 5% if compared with the Planck data. It is easy to obtain the integral

$$H_0^{(\infty)} = \frac{1}{T_0}\int_0^\infty \frac{dz'}{(1+z')E(z')}. \tag{25}$$

This approximation is mandatory in view to justify our approach. Clearly, considering only the first-order term, we recover the parameterization

$$T(z) = \frac{T_0}{(1+z)} = a(t)T_0\,, \tag{26}$$

that allows us to label the universe age at various redshifts $T(z)$ starting from T_0. The definition of look-back time can be recast as:

$$H_0 = \frac{1}{T_{lt}(z)}\int_0^z \frac{dz'}{(1+z')E(z')}. \tag{27}$$

According to this equation, we can infer H_0 from $T_{lt}(z)$ at any z. This result is consistent with the age of the Universe, by considering the general definition

$$T_{lt}(z) = T_0 - T(z)\,, \tag{28}$$

where T_0 and $T(z)$ are the Universe age, today and at a given redshift, respectively. Considering Equation (26), we can derive

$$H_0^{(z)} = \frac{(1+z)}{T_0 z}\int_0^z \frac{dz'}{(1+z')E(z')}. \tag{29}$$

Equation (26) can be confronted with other parameterizations. The idea is linking different ages of the Universe with today's epoch, avoiding the integral time evolution, depending on $E(z)$, as in Equation (29). In other words, one can adopt a point-by-point labeling process. The most natural label that we may use is the scaling factor itself $a(t)$, which expresses how the size of the Universe changes with its expansion. In this perspective, $T(z)$ is a projection of T_0 at a given redshift. This is the main reason why we have operatively computed this labeling from Equation (24).

As noted in [90], for $z \to +\infty$, it is $\lim_{z\to+\infty} \frac{z+1}{z} = 1$, and thus it is easy to recover Equation (25) from our approach, which can also be interpreted as the definition of Universe age, denoted as T_0. This means that the parameterization is in agreement with the age definition at high values of z. Additionally, in Ref. [90], it is demonstrated that this parameterization is remarkably consistent with different H_0 measurements, ranging from late and early epochs, where different probes are taken into account. More specifically, we report here results obtained by the Planck collaboration for the following quantities [1]:

$$T_0 = 13.797\,\text{Gyr}, \quad \Omega_r = 9.252\times10^{-5}, \quad \Omega_M = 0.3153, \quad \Omega_\Lambda = 0.6847. \tag{30}$$

which have been compared with the following H_0 observations at 68% CL:

- $H_0 = 73.04 \pm 1.04$ km/(s Mpc) from the SH0ES collaboration, inferred by the cosmic distance ladder method considering Classical Cepheids + SNe Ia up to $z = 0.15$ [24];
- $H_0 = 67.4 \pm 0.5$ km/(s Mpc) from the Planck collaboration, obtained by the CMBR observations at $z \sim 1100$ [1];
- $H_0 = 69.9 \pm 1.9$ km/(s Mpc), obtained by using the TRGB as an anchor for SNe Ia instead of the Classical Cepheids, at $z = 0.08$ [127];
- $H_0 = 75.8 \pm 5.0$ km/(s Mpc), derived from SNe Type II as the last step of the cosmological ladder, at $z = 0.45$ [128];
- $H_0 = 73.3 \pm 4.0$ km/(s Mpc), derived from the Mira Variables employed as anchors of SNe Ia, at $z \sim 0.15$ [276];
- $H_0 = 76.0 \pm 2.6$ km/(s Mpc), derived from the Tully-Fisher relation for spiral galaxies, at $z = 0.5$ [129];
- $H_0 = 73.3 \pm 2.5$ km/(s Mpc), derived from the surface brightness fluctuations for the galaxies, at $z = 0.33$ [130];
- $H_0 = 69.5 \pm 3.3$ km/(s Mpc), inferred from the Large Scale Structure t_{eq} standard ruler, and thus confronted to our computations at the redshift of equivalence $z_{eq} \sim 3300$ [277];
- $H_0 = 72.0 \pm 1.9$ km/(s Mpc), inferred from the masers + SNe Ia and compared at $z \sim 0.15$ [100];
- $H_0 = 73.3 \pm 1.8$ km/(s Mpc), derived from gravitational lensed quasars, confronted at $z = 0.745$ [153];
- $H_0 = 67.9 \pm 1.5$ km/(s Mpc), which is a measurement provided by the CMBR independently from the Planck collaboration, and as such corresponding at the reionization epoch $z \sim 1100$ [159];
- $H_0 = 69.6 \pm 2.1$ km/(s Mpc), linked to the 21 cm absorption line and corresponding at the beginning of the so-called Cosmic Dawn, i.e., when the first stars formed ($z \sim 17.2$), in combination with CMBR data and considering a Chaplygin gas model for the dark sector [278];
- $H_0 = 73.4 \pm 8.8$ km/(s Mpc), deduced by gravitational waves, at $z = 0.438$ [189].

We remind that the corresponding redshift for each measurement has been determined by considering either the upper limit of the redshift range of the sample used to infer H_0 or the redshift associated with the specific physical process.

Results reported in [90] are displayed in left panel of Figure 2. They will be used as reference for our tests. Here, we consider also the effects of 5% approximation in assuming $H_0 = 1/T_0$. Essentially, error bands at 5% can be taken into account. Results are shown in the right panel of Figure 2, where we see that the model is still consistent with the H_0 measurements. We have also performed a polynomial fit of the H_0 measurements, independent of the cosmological model. It is worth noticing that it is consistent with late and early measurements, while it results shifted with respect to the peak. This feature has to be expected due to the lack of direct H_0 in the intermediate redshift range.

It is important to discuss the value of T_0 used in the analysis. This quantity is linked to H_0. More specifically, an anti-correlation exists between T_0 and H_0 has been reported in Ref. [279]. An independent way to test H_0 is to compare measurements with estimate ages of old objects such as stars and globular clusters.

In this sense, different measurements are consistent with T_0 derived from early-type observations [191,280–283]. This suggests that the H_0 value, inferred from late-type observations, would imply a Universe that is too young according to these measurements. Therefore, novel physics might be required to reconcile H_0 with the late-type derivations.

This is the first reason why we started from the values provided by the Planck Collaboration. The second one is that both T_0 and H_0, according to Planck, are derived quantities which have been computed by the six aforementioned free parameters. Therefore, even if T_0 and H_0 are linked, we do not incur in a circularity problem [1].

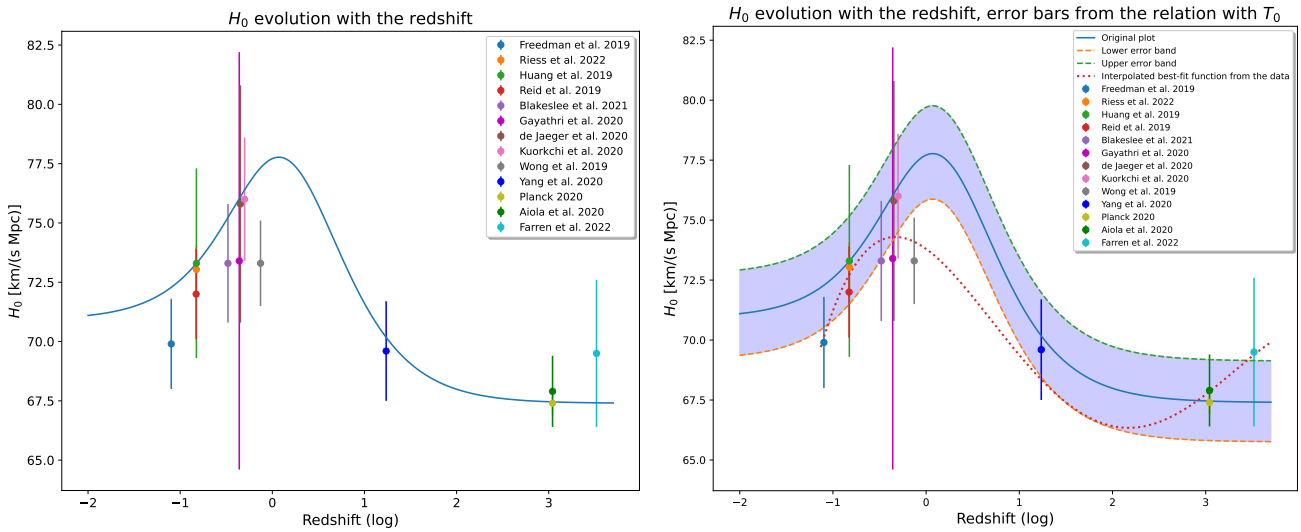

Figure 2. (**Left panel**) The values of H_0 derived from Equation (29) are plotted against the redshift and confronted with observational data [90]. For each measurement, the redshift value has been selected either at the upper limit of the redshift range of the sample or at the redshift corresponding to the specific physical phenomenon considered for the estimation (cosmic dawn, recombination, equivalence epoch, and so on). (**Right panel**) the same plots, but considering a 5% uncertainty on our model linked to the relation between T_0 and H_0, and also a polynomial fit on the H_0 measurements. The x-axis is reported in a logarithmic scale. We recall that the measurements have been taken from [1,24,100,127–130,153,159,189,276–278]

Considering Equation (24), it is easy to see that the first order expansion works at low redshifts but it should decrease in efficiency at higher values of z. Notably, from Equation (25), we recover T_0 at higher redshifts. Furthermore, we may note that the evolution of $a(t)$, depending on the given cosmological eras dominated by different densities, is quite similar to a linear behavior, as shown in Figure 3. Here, we compare the evolution of $a(t)$, obtained by a 9th- degree polynomial fit, with a straight line. We may note that the two curves are remarkably similar for a large range of $T(z)$ values and easily converge to the above limit of H_0^z at high redshifts.

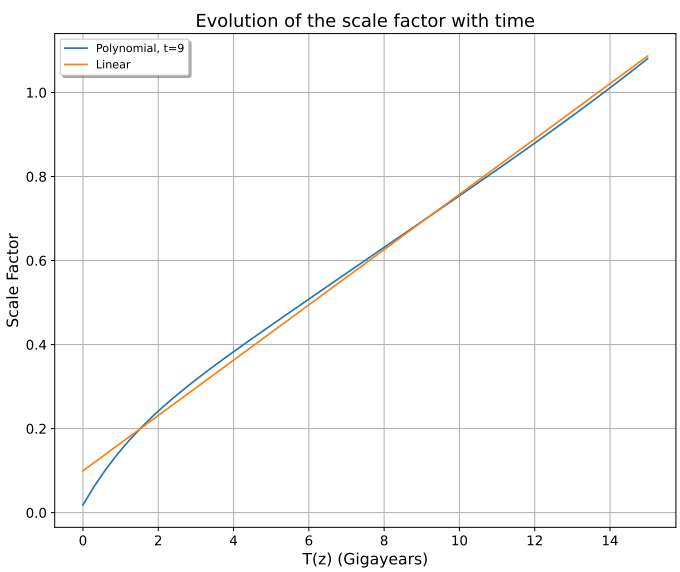

Figure 3. Evolution of the scale factor $a(t)$ with time. The blue curve represents the best fit using a 9th-degree polynomial to reproduce its numerical evolution as precisely as possible, while the orange curve is the fit with a straight line.

To further validate our claims, we can try different parameterizations, which may be derived from different assumptions on the dominating cosmological densities in the function $E(z)$. This means that we do not consider our labeling, but specific approximations of the cosmological models. By taking into account the definition on $T(z)$ in Equation (14), via the time-evolution integral, one can derive

$$T(z) = \frac{1}{H_0} \int_z^\infty \frac{dz'}{(1+z')E(z')}. \tag{31}$$

In general, this integral has to be solved numerically, but it is possible to find simple analytical formulas linking it to T_0 for specific approximations of $E(z)$. Let us start from a matter-dominated Universe. In this case, it is $E(z) = \sqrt{\Omega_M(1+z)^3}$, from which $T(z)$ becomes

$$T(z) = \frac{1}{H_0} \int_z^\infty \frac{dz'}{(1+z')^{5/2}}. \tag{32}$$

It can be solved analytically and one finds that the following parameterization is exactly valid [284]:

$$T(z) = \frac{T_0}{(1+z)^{3/2}}. \tag{33}$$

If we introduce this new parameterization into our equations and compare the derived $H_0^{(z)}$ with the actual measurements, we obtain results shown in the left panel of Figure 4. It is worth noticing that this approach does not perform well in this case, as it produces a theoretical curve for H_0 that yields unreasonable results for low values of z, and it is not consistent with the late-type measurements, even for redshift regions where the Universe may be considered matter-dominated.

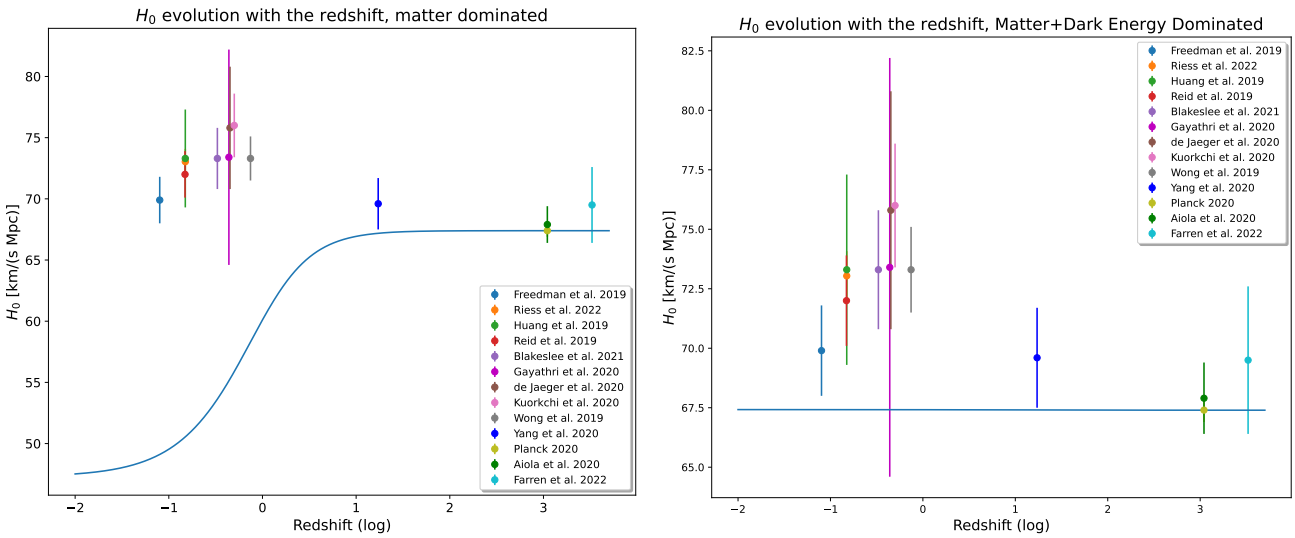

Figure 4. **(Left panel)** the value of H_0 derived considering $T(z) = \frac{T_0}{(1+z)^{3/2}}$ as a function of the redshift, confronted with observational data. (**Right Panel**) the same comparison, but with a parameterization consistent with the Universe dominated by matter and dark energy. The x-axis is in logarithmic scale. We recall that the measurements have been taken from [1,24,100,127–130,153,159,189,276–278]

If we, instead, consider a flat Universe with only dark energy and matter components (that is what we observe for the vast majority of the Universe lifetime, neglecting the radiation contribution), it is $E(z) = \sqrt{\Omega_M(1+z)^3 + \Omega_\Lambda}$. We find, starting from the equations derived in [285] for this particular case, that $T(z)$ can be expressed as

$$T(z) = \frac{2}{3H_0}\left(1 + \frac{\Omega_M}{\Omega_\Lambda}\right)^{1/2} \sinh^{-1}\left[\left(\frac{\Omega_\Lambda}{\Omega_M}\right)^{1/2}(1+z)^{-3/2}\right]. \tag{34}$$

From this equation, T_0 can be easily recovered in the limit $z \to 0$. In other words, the relation between $T(z)$ and T_0 is as follows:

$$T(z) = \frac{\sinh^{-1}\left[\left(\frac{\Omega_\Lambda}{\Omega_M}\right)^{1/2}(1+z)^{-3/2}\right]}{\sinh^{-1}\left[\left(\frac{\Omega_\Lambda}{\Omega_M}\right)^{1/2}\right]} T_0. \tag{35}$$

By introducing the last equation in our approach, we obtain the results shown in the right panel of Figure 4. We observe that the derived estimate for H_0^z is independent of the redshift and aligns with the measurements provided by the Planck collaboration. However, it is not consistent with measurements of H_0 obtained at lower redshifts. It is worth noticing that this estimate depends on the ratio Ω_Λ/Ω_M, which, in our case, is fixed to the values provided by Planck, but can be modified for other inferred values of these quantities.

As additional case, we have considered a radiation-dominated Universe, where $E(z) = \sqrt{\Omega_r(1+z)^4}$ and

$$T(z) = \frac{T_0}{(1+z)^2}. \tag{36}$$

Furthermore, without any assumption, we can directly use the integral definitions of $T(z)$ and T_0. The plots of these two cases are shown in Figure 5.

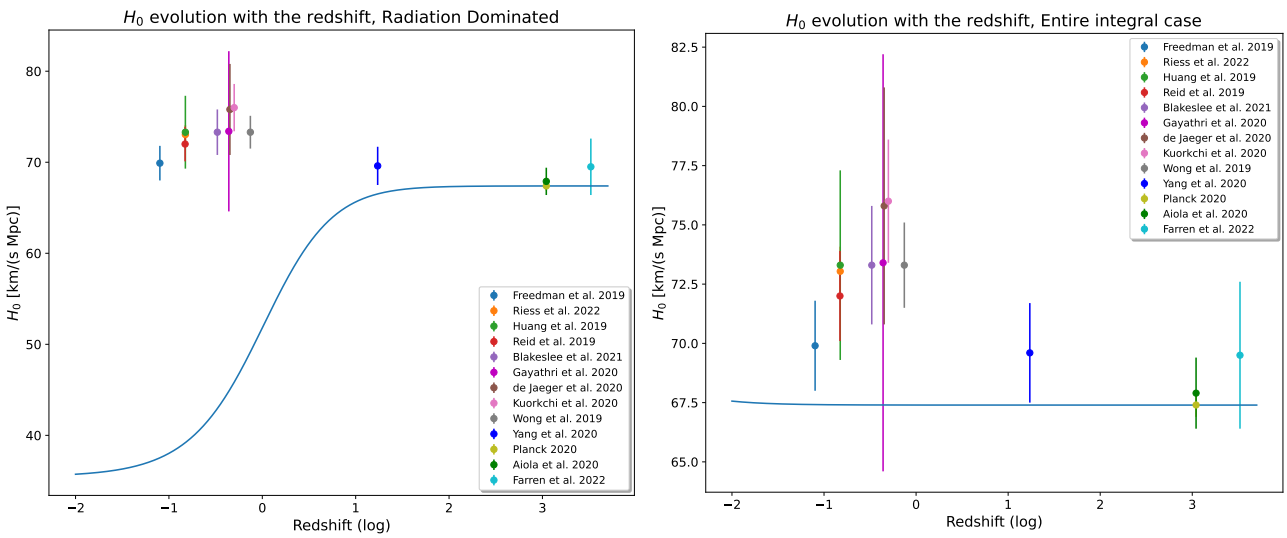

Figure 5. **(Left panel)** The value of H_0 derived from $T(z) = \frac{T_0}{(1+z)^2}$, plotted against the redshift and compared with observational data. (**Right panel**) The same comparison, but taking into account the integral definitions of T_0 and $T(z)$. The x-axis is in logarithmic scale. We recall that the measurements have been taken from [1,24,100,127–130,153,159,189,276–278]

The result obtained for the radiation-dominated Universe is reported in the left panel. Notably, we observe unreasonable values for H_0 even with respect to the matter-dominated case. On the right panel, we show the result obtained adopting the general integral for $T(z)$, that is Equation (31). Here, we obtain a constant value for H_0 around 67.4 km/(s Mpc), independent of the redshift. This is because, by adopting the integral, we fall into a circularity problem which gives the H_0 provided by the Planck Collaboration at all redshifts. This result is also remarkably consistent with the one obtained by Equation (35) for the Universe dominated by dark energy and matter.

Interestingly, we emphasize that the parameterization presented in Equation (26) is the only one consistent with both early and late-type measurements. In this framework, it can be exactly derived from an empty Universe with $E(z) = \sqrt{\Omega_k(1+z)^2}$. However, it is essential to note that such a Universe is in severe disagreement with cosmological

observations [1]. This discrepancy highlights the conceptual difference between our labeling approach and the derivation of $T(z)$ through the integral in Equation (31).

In summary, the parameterization shown in Equation (26) has been chosen as a labeling process connecting the age of the Universe at various epochs through a point-by-point approach. Mathematically, it can be derived from a reliable approximation of the scale factor as a function of time, working also for high-redshift. Among the different tests, it stands out as the only parameterization that aligns with the H_0 observations at both early and late epochs. It is worth stressing that, apart our labelling $T(z)$, the other tests have been performed considering other parameterizations. This does not exclude the possibility of choosing other relations between $T(z)$ and T_0 which involve more complex functions as $T(z) = T_0/(1 + P(z))$ where $P(z)$ can be some function of the redshift (e.g., a polynomial) as considered in cosmography [2]. From this more general approach, one could obtain realistic models capable of matching better the cosmic history.

4.2. A Variable H_0 from Late-Type Estimates

The look-back time parameterization of H_0 can be compared with late-type measurements for the cosmological parameters Ω_M and Ω_Λ. For this comparison, we will use results obtained by the cosmological ladder approach involving the SNe Ia of the Pantheon+ set [115,116]. In particular, we consider two different sets of results regarding Ω_M and Ω_Λ. In both cases, we use the value for T_0 provided by the Planck results, since an estimate for this quantity cannot be derived directly from the cosmological computations reported in Ref. [116]. For the first set, we start from the values obtained in [116] for a flat ΛCDM model where they imposed $\Omega_M + \Omega_\Lambda = 1$. They found

$$\Omega_M = 0.334 \pm 0.018, \quad \Omega_\Lambda = 0.666 \pm 0.018. \tag{37}$$

Considering the best-fit values of these quantities in our model, and comparing the results with the aforementioned H_0 measurements, we find the results displayed in the left panel of Figure 6. We note how, in general, the curve obtained by our model is consistent with the majority of the H_0 measurements. However, we notice an interesting tension with the measurement provided by the Planck collaboration, which is, instead, remarkably matched by the curve displayed in Figure 2.

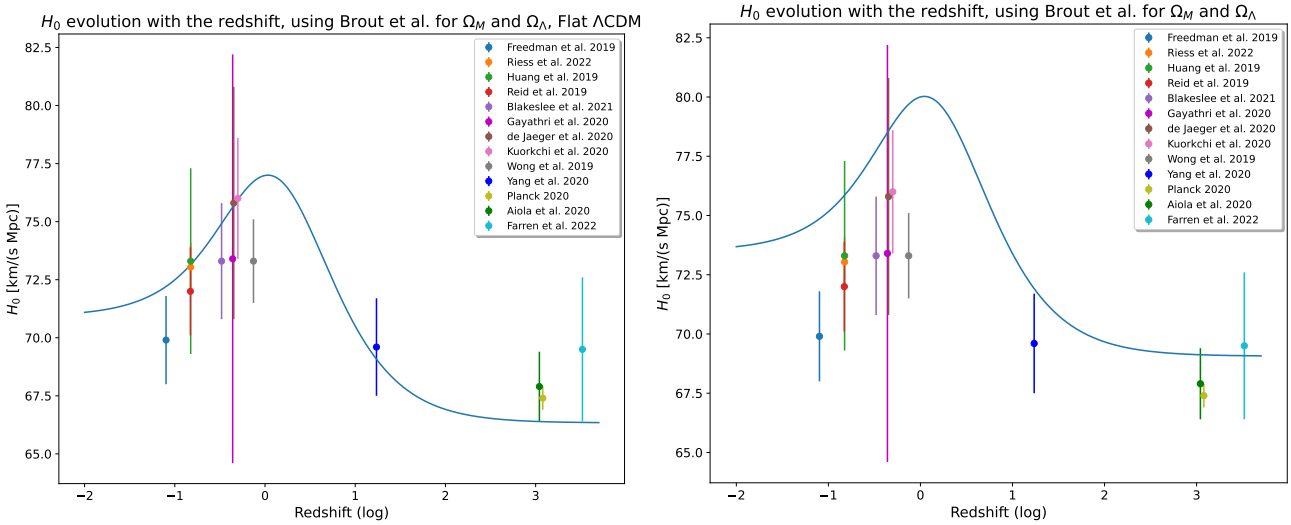

Figure 6. (**Left panel**) the value of H_0 derived from our methodology considering $T(z) = \frac{T_0}{(1+z)}$ plotted against the redshift and compared with observational data, starting from the Pantheon+ results for a flat ΛCDM model. (**Right panel**) the same comparison, but relaxing the flatness assumption. The x-axis is in logarithmic scale. We recall that the measurements have been taken from [1,24,100,127–130,153,159,189,276–278].

Indeed, we note how, at high redshift, the value for H_0 provided by this model decreases to 66.34 km/(s Mpc), which is more than 2σ in tension with the Planck measurement. An interesting observation is that this value is smaller than the measured one, contrary to what would be expected, given that late-type measurements usually translate with higher estimates for H_0.

From this, we may conclude that the different values provided for Ω_M and Ω_Λ from early and late-type measurements have a significant impact on the comparison of our model with measurements.

This conclusion is further supported by the second case we have considered, in which we have taken into account the results for Ω_M and Ω_Λ obtained in [116] relaxing the flatness assumption for the ΛCDM, for which

$$\Omega_M = 0.306 \pm 0.057, \quad \Omega_\Lambda = 0.625 \pm 0.084, \tag{38}$$

while for the value of Ω_r, we rely on the value provided by Planck. Using our model for these starting values, we derive the right panel of Figure 6. We observe a shift towards higher values of H_0 with respect to the results obtained in the left panel of the same figure and note that the curve is inconsistent with many observations, particularly those concerning the late Universe. In this comparison, it is important to point out the large uncertainties on Ω_M and Ω_Λ values, which could play a significant role.

5. A Variable H_0 in ΛCDM Model

Let us discuss now the implications of our approach in the context of ΛCDM model. As previously mentioned, a variable H_0 can be interpreted as a possible hint for the breakdown of FLRW metric and the ΛCDM model [75,155]. Such a variation can be explained in the context of ETGs [29,81]. However, our analysis reveals that a variable H_0 can be entirely derived within the framework of ΛCDM model, starting from some fundamental concepts and from the parameterization in Equation (26), without making any a priori assumption on the evolution of H_0. This finding does not contradict the role of H_0 in the Friedman equations because the variation of this constant is strictly connected to the redshift at which it has been measured.

A robust confirmation of such a hypothesis would be attainable by conducting independent measurements within the intermediate redshift range, where we observe the peak in our H_0 estimate as shown in Figure 2.

Notably, the Pantheon and Pantheon+ SNe Ia datasets [115,117], spanning up to $z = 2.26$, encompass a broad redshift range, albeit with a majority of SNe Ia situated in the low-redshift region. H_0 estimates already exist in this range, (e.g., [175,209,214]) but depend on calibration processes involving probes at lower redshifts. Consequently, promising new insights are anticipated from forthcoming investigations utilizing novel probes, such as quasars, gravitational wave standard sirens, galaxy clusters, Lyman-α lines, or GRBs (as reported in [186,210,211,215,286,287]).

In this context, the Euclid Mission [288,289] could play a pivotal role. While its main focus is investigating the nature of dark energy via a wide set of observations of galaxy clusters and weak lensing phenomena [290] by also testing possible modifications of GR [291,292], it also holds the potential to provide precise estimates of cosmological parameters like H_0 within the intermediate redshift range. Additionally, given the wide survey expected by Euclid, even though not primarily centered on transient phenomena such as SNe Ia, is likely to contribute significantly also to these types of observations [293].

Let us discuss now the implications of a variable H_0 on the cosmological observations. To achieve this, we have investigated, as an example, how luminosity and light-travel distances behave with the H_0^z function in Equation (27), and compared these distances with the results obtained by assuming the fixed values measured by the SH0ES and Planck collaborations. We selected the first distance because it is arguably the most relevant for cosmological measurements, and the second due to its connection with the look-back

time. It is worth noticing that similar considerations apply to other cosmological distances. The results are presented in Figure 7.

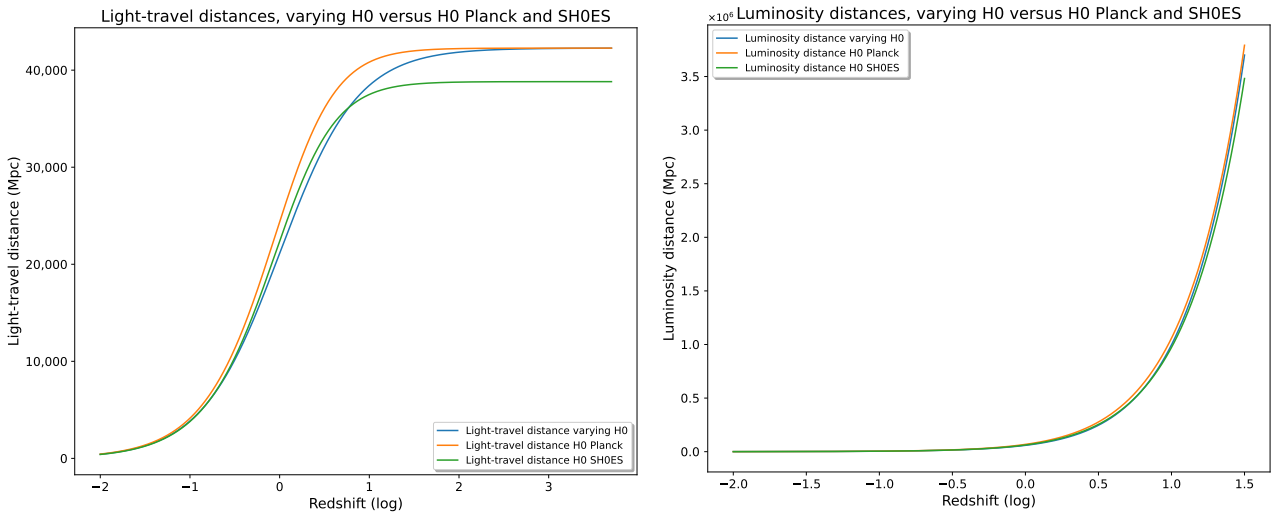

Figure 7. (**Left panel**) a comparison between the light-travel distance computed using the H_0^z function (Equation (27)), with the distances derived by using the fixed values for H_0 provided by the SH0ES and Planck collaborations. (**Right panel**) the same comparison as in the left panel, but considering the luminosity distance. The x-axis is in logarithmic scale for both panels. Note that there are different scales on the x-axis in the two plots.

Both panels in this figure demonstrate how our approach naturally connects the two distances derived from fixed values of H_0 without significantly changing the overall behavior in the investigated redshift range. The effect is particularly evident in the left panel, where the light-travel distance is represented. We see how the distance computed by our approach is similar to the one derived from the SH0ES observations, converging towards the Planck results at higher redshifts. This can be attributed to the role of H_0, which is a normalization constant, not linked to any astrophysical source. In conclusion, while a variable H_0 does impact the definitions of cosmological distances, it neither substantially changes the conclusions drawn from our method, especially at lower redshifts, nor it changes the value of the distances so that it could be in contrast with observations.

6. Discussion and Conclusions

In this work, we provided, without claiming for completeness, a summary of H_0 measurements in both early and late-type frameworks, highlighting the existence of a tension independent of the particular probe or methodology used. This independence emphasizes the decreasing probability that the tension stems from potential instrument-related biases or unaddressed systematic effects.

We explored how this tension has been tackled in the context of new physics, beyond the ΛCDM model. Various approaches have been proposed, yielding promising results. However, the main problem is the substantial degeneracy among the different proposed frameworks, which does not allow us, up to now, to define a unique and definitive extension of the ΛCDM model. From this point of view, it is crucial to understand that, whichever the extended framework may be, it has to be able to reproduce the ΛCDM results where the concordance among the vast majority of measurements is evident. This check is essential in view to recover self-consistent models in agreement with cosmic history.

A recent approach has brought significant attention to the possibility of a "running H_0" [75], both in the observations context and in the interpretation of a quantity that is traditionally regarded as "constant".

In this framework, we reported the analysis performed in [90], which defines the Hubble constant via the look-back time. It is possible to provide a general formula consistent

with the measurements of this quantity both at early and late epochs just considering the related look-back time measurement of H_0 at any epoch. Here, we delve further into this direction starting from Equation (26) and discussing the consequences on the various cosmological distances.

Specifically, we highlight that the formula $T(z) = T_0/(1+z)$ arises naturally through a point-by-point labeling of the age of the Universe at different redshifts, without the need to account for the cosmological evolution already incorporated into the function $E(z)$.

To validate our assumption, we show how it can be mathematically derived from a reliable approximation of the scale factor $a(t)$, and how other parameterizations, which can be derived from specific assumptions on the densities at various epochs, do not effectively fit observational measurements of H_0.

We have also considered different values of Ω_M and Ω_Λ, taken by late-type results from the SH0ES + Pantheon + sets, finding significant effects in our comparisons, particularly regarding the value for H_0 provided by the Planck collaboration, which is not recovered in these cases. This observation is interesting because it allows us to conclude that the different measurements of Ω_M and Ω_Λ, for late and early epochs, introduce a notable tension.

In particular, we derived the light-travel and luminosity distances as functions of our variable H_0 and compared the results with those obtained using the fixed values provided by early and late-time measurements. We found that, by our new definition, it is possible to obtain distances able to link the SH0ES and Planck distances, without significantly modifying their overall behavior. In our opinion, this is an important check because the absence of unreasonable results, starting from different distance definitions, confirms the reliability of the approach.

An issue that may arise pertains to the measurements of the aforementioned $H(z)$ function and the extrapolation to the H_0 value. In fact, one should be able to discern between variations related to the functional form of $H(z)$ and the variable nature of H_0 at different redshifts.

An important point that must be emphasized is that our results have been achieved entirely within the framework of the ΛCDM scenario, without requiring modifications or extensions. Theoretically, a variable H_0 can be interpreted as a breakdown of the FLRW metric. In our case, H_0 is an integration constant related to the size of the Universe at a given redshift. In other words, the value of H_0 could depend on the redshift at which it is measured, thus not undermining its role in the cosmological equations but removing the tension issue. It is worth noticing how a better fit with respect to the measurements can be obtained by starting from the early estimate of densities rather than the late ones. However, this does not exclude the necessity of extending GR and ΛCDM model, given other issues like the nature of dark energy and dark matter, and the lack of a self-consistent Quantum Gravity theory [29].

Observationally, H_0 tension is not the only tension in cosmology [25]. For example, there is the so-called $S_8 = \sigma_8\sqrt{\Omega_M/0.3}$ tension, where S_8 is a parameter indicating the strength with which matter is clustered in the Universe. On this parameter, a discrepancy at $2-3\sigma$ level [25] exists between the measurements inferred by the Planck data and low-redshift probes, such as the weak gravitational lens and clusters of galaxies [294,295]. It is essential to investigate whether similar considerations to those discussed above can also apply to S_8 or if it represents an independent signal of deviations from the cosmological Standard Model.

Furthermore, other measurements challenge the ΛCDM model, like some evidence of a possible non-zero curvature of the Universe [296], as well as anomalies in CMB observations, i.e., apparent correlations between the Solar System plane and certain aspects of CMB. This evidence seems to provide a preferred reference position which should not be possible if the Cosmological Principle is always valid [297–299].

In conclusion, our analysis suggests that new physics, in the form of extensions or modifications to ΛCDM model, may not be necessary to address the specific issue of H_0

tension, but it does not exclude its necessity for other fundamental issues. In a forthcoming study, we will discuss the other tensions under the standard of look-back time approach.

Author Contributions: Conceptualization, S.C. and G.S.; Methodology, G.S. and G.D.S.; Formal analysis, S.C. and G.D.S.; Investigation, G.D.S.; Data curation, G.S.; Writing—original draft, S.C. All authors have read and agreed to the published version of the manuscript.

Funding: This research received no external funding.

Data Availability Statement: Data are contained within the article.

Acknowledgments: This paper is based upon work from the COST Action CA21136, "Addressing observational tensions in cosmology with systematics and fundamental physics" (CosmoVerse) supported by COST (European Cooperation in Science and Technology). The authors acknowledge the support by Istituto Nazionale di Fisica Nucleare, Sez. di Napoli, Iniziativa Specifica QGSKY. The authors express their gratitude for valuable and constructive discussions to Giada Bargiacchi, Micol Benetti, Eoin Colgain, Maria Giovanna Dainotti, David Kraljic, Stefan Ruester, Shahin Sheikh-Jabbari, and Alessandro D.A.M. Spallicci. Finally, we want to thank the anonymous referees for their feedback and useful suggestions.

Conflicts of Interest: The authors declare no conflict of interest.

References

1. Aghanim, N.; Akrami, Y.; Ashdown, M.; Aumont, J.; Baccigalupi, C.; Ballardini, M.; Banday, A.J.; Barreiro, R.B.; Bartolo, N.; Basak, S.; et al. Planck 2018 results. *Astron. Astrophys.* **2020**, *641*, A6. [CrossRef]
2. Weinberg, S. *Gravitation and Cosmology: Principles and Applications of the General Theory of Relativity*; John Wiley and Sons: New York, NY, USA, 1972.
3. Guth, A.H. Inflationary universe: A possible solution to the horizon and flatness problems. *Phys. Lett. D* **1981**, *23*, 347–356. [CrossRef]
4. Starobinsky, A. Spectrum of relict gravitational radiation and the early state of the universe. *J. Exp. Theor. Phys. Lett.* **1979**, *30*, 682–685.
5. Particle Data Group; Zyla, P.; Barnett, R.M.; Beringer, J.; Dahl, O.; Dwyer, D.A.; Groom, D.E.; Lin, C.J.; Lugovsky, K.S.; Pianori, E.; et al. Review of particle physics. *Progr. Theor. Exp. Phys.* **2020**, *2020*, 083C01.
6. Particle Data Group; Workman, R.L.; Burkert, V.D.; Crede, V.; Klempt, E.; Thoma, U.; Tiator, L.; Agashe, K.; Aielli, G.; Allanach, B.C.; et al. Review of particle physics. *Prog. Theor. Exp. Phys.* **2022**, *2022*, 083C01. [CrossRef]
7. Riess, A.G.; Filippenko, A.V.; Challis, P.; Clocchiatti, A.; Diercks, A.; Garnavich, P.M.; Gilliland, R.L.; Hogan, C.J.; Jha, S.; Kirshner, R.P.; et al. Observational Evidence from Supernovae for an Accelerating Universe and a Cosmological Constant. *Astron. J.* **1998**, *116*, 1009–1038. [CrossRef]
8. Riess, A.G.; Strolger, L.G.; Casertano, S.; Ferguson, H.C.; Mobasher, B.; Gold, B.; Challis, P.J.; Filippenko, A.V.; Jha, S.; Li, W.; et al. New Hubble Space Telescope Discoveries of Type Ia Supernovae at z $\geq$ 1: Narrowing Constraints on the Early Behavior of Dark Energy. *Astrophys. J.* **2007**, *659*, 98–121. [CrossRef]
9. Perlmutter, S.; Aldering, G.; Goldhaber, G.; Knop, R.A.; Nugent, P.; Castro, P.G.; Deustua, S.; Fabbro, S.; Goobar, A.; Groom, D.E.; et al. Measurements of Ω and Λ from 42 High-Redshift Supernovae. *Astrophys. J.* **1999**, *517*, 565–586. [CrossRef]
10. Bahcall, N.A.; Ostriker, J.P.; Perlmutter, S.; Steinhardt, P.J. The Cosmic Triangle: Revealing the State of the Universe. *Science* **1999**, *284*, 1481–1488. [CrossRef]
11. Spergel, D.N.; Verde, L.; Peiris, H.V.; Komatsu, E.; Nolta, M.R.; Bennett, C.L.; Halpern, M.; Hinshaw, G.; Jarosik, N.; Kogut, A.; et al. First-Year Wilkinson Microwave Anisotropy Probe (WMAP) Observations: Determination of Cosmological Parameters. *Astrophys. J. Suppl. Ser.* **2003**, *148*, 175–194. [CrossRef]
12. Schimd, C.; Tereno, I.; Uzan, J.P.; Mellier, Y.; van Waerbeke, L.; Semboloni, E.; Hoekstra, H.; Fu, L.; Riazuelo, A. Tracking quintessence by cosmic shear. *Astron. Astrophys.* **2006**, *463*, 405–421. [CrossRef]
13. McDonald, P.; Seljak, U.; Burles, S.; Schlegel, D.J.; Weinberg, D.H.; Cen, R.; Shih, D.; Schaye, J.; Schneider, D.P.; Bahcall, N.A.; et al. The Lyα Forest Power Spectrum from the Sloan Digital Sky Survey. *Astrophys. J. Suppl. Ser.* **2006**, *163*, 80–109. [CrossRef]
14. Bamba, K.; Capozziello, S.; Nojiri, S.; Odintsov, S.D. Dark energy cosmology: The equivalent description via different theoretical models and cosmography tests. *Astrophys. Space Sci.* **2012**, *342*, 155–228. [CrossRef]
15. Joyce, A.; Jain, B.; Khoury, J.; Trodden, M. Beyond the cosmological standard model. *Phys. Rep.* **2015**, *568*, 1–98. [CrossRef]
16. Abbott, T.M.C.; Allam, S.; Andersen, P.; Angus, C.; Asorey, J.; Avelino, A.; Avila, S.; Bassett, B.A.; Bechtol, K.; Bernstein, G.M.; et al. First Cosmology Results using Type Ia Supernovae from the Dark Energy Survey: Constraints on Cosmological Parameters. *Astrophys. J.* **2019**, *872*, L30. [CrossRef]
17. Salucci, P.; Esposito, G.; Lambiase, G.; Battista, E.; Benetti, M.; Bini, D.; Boco, L.; Sharma, G.; Bozza, V.; Buoninfante, L.; et al. Einstein, Planck and Vera Rubin: Relevant Encounters Between the Cosmological and the Quantum Worlds. *Front. Phys.* **2021**, *8*, *579* . [CrossRef]

18. Zwicky, F. Die Rotverschiebung von extragalaktischen Nebeln. *Helv. Phys. Acta* **1933**, *6*, 110–127.
19. Babcock, H.W. The rotation of the Andromeda Nebula. *Lick Obs. Bull.* **1939**, *498*, 41–51. [CrossRef]
20. Rubin, V.C.; Ford, V.K. Rotation of the Andromeda Nebula from a Spectroscopic Survey of Emission Regions. *Astrophys. J.* **1970**, *159*, 379. [CrossRef]
21. Schnee, R.W. Introduction to dark matter experiments. In *Physics of the Large and the Small: TASI 2009*; Csaki, C., Dodelso, S., Eds.; World Scientific Publishing Co. Pte. Ltd.: Singapore, 2011; pp. 775–829. [CrossRef]
22. Mitsou, V.A. Overview of searches for dark matter at the LHC. *J. Phys. Conf. Ser.* **2015**, *651*, 012023. [CrossRef]
23. Aprile, E.; Aalbers, J.; Agostini, F.; Alfonsi, M.; Amaro, F.D.; Anthony, M.; Antunes, B.; Arneodo, F.; Balata, M.; Barrow, P.; et al. The XENON1T dark matter experiment. *Eur. Phys. J. C* **2017**, *77*, 881. [CrossRef]
24. Riess, A.G.; Yuan, W.; Macri, L.M.; Scolnic, D.; Brout, D.; Casertano, S.; Jones, D.O.; Murakami, Y.; Anand, G.S.; Breuval, L.; et al. A Comprehensive Measurement of the Local Value of the Hubble Constant with 1 km/s/Mpc Uncertainty from the Hubble Space Telescope and the SH0ES Team. *Astrophys. J. Lett.* **2022**, *934*, L7. [CrossRef]
25. Abdalla, E.; Abellán, G.F.; Aboubrahim, A.; Agnello, A.; Akarsu, Ö.; Akrami, Y.; Alestas, G.; Aloni, D.; Amendola, L.; Anchordoqui, L.A.; et al. Cosmology intertwined: A review of the particle physics, astrophysics, and cosmology associated with the cosmological tensions and anomalies. *J. High Energy Astrophys.* **2022**, *34*, 49–211. [CrossRef]
26. Moresco, M.; Amati, L.; Amendola, L.; Birrer, S.; Blakeslee, J.P.; Cantiello, M.; Cimatti, A.; Darling, J.; Valle, M.D.; Fishbach, M.; et al. Unveiling the Universe with emerging cosmological probes. *Living Rev. Relativ.* **2022**, *25*, 6. [CrossRef]
27. Capozziello, S. Curvature Quintessence. *Int. J. Mod. Phys. D* **2002**, *11*, 483–491. [CrossRef]
28. Nojiri, S.; Odintsov, S.D. Unified cosmic history in modified gravity: From $F(R)$ theory to Lorentz non-invariant models. *Phys. Rep.* **2011**, *505*, 59–144. [CrossRef]
29. Capozziello, S.; Laurentis, M.D. Extended Theories of Gravity. *Phys. Rep.* **2011**, *509*, 167–321. [CrossRef]
30. Capozziello, S.; Laurentis, M.D.; Odintsov, S.; Stabile, A. Hydrostatic equilibrium and stellar structure in $f(R)$-gravity. *Phys. Rev. D* **2011**, *83*, 064004. [CrossRef]
31. Nojiri, S.; Odintsov, S.; Oikonomou, V. Modified gravity theories on a nutshell: Inflation, bounce and late-time evolution. *Phys. Rep.* **2017**, *692*, 1–104. [CrossRef]
32. Felice, A.D.; Tsujikawa, S. $f(R)$ Theories. *Living Rev. Relativ.* **2010**, *13*, 3. [CrossRef]
33. Hu, W.; Sawicki, I. Models of $f(R)$ Cosmic Acceleration that Evade Solar-System Tests. *Phys. Rev. D* **2007**, *76*, 064004. [CrossRef]
34. Capozziello, S.; Cardone, V.F.; Troisi, A. Reconciling dark energy models with $f(R)$ theories. *Phys. Rev. D* **2005**, *71*, 043503. [CrossRef]
35. Oikonomou, V. Effects of a pre-inflationary de Sitter bounce on the primordial gravitational waves in $f(R)$ gravity theories. *Nucl. Phys. B* **2022**, *984*, 115985. [CrossRef]
36. Capozziello, S.; D'Agostino, R.; Luongo, O. Extended Gravity Cosmography. *Int. J. Mod. Phys. D* **2019**, *28*, 1930016. [CrossRef]
37. Bajardi, F.; D'Agostino, R.; Benetti, M.; De Falco, V.; Capozziello, S. Early and late time cosmology: The $f(R)$ gravity perspective. *Eur. Phys. J. Plus* **2022**, *137*, 1239. [CrossRef]
38. Cai, Y.F.; Capozziello, S.; De Laurentis, M.; Saridakis, E.N. $f(T)$ teleparallel gravity and cosmology. *Rep. Prog. Phys.* **2016**, *79*, 106901. [CrossRef] [PubMed]
39. Benetti, M.; Capozziello, S.; Lambiase, G. Updating constraints on $f(T)$ teleparallel cosmology and the consistency with big bang nucleosynthesis. *Mon. Not. R. Astron. Soc.* **2021**, *500*, 1795–1805. [CrossRef]
40. Nojiri, S.; Odintsov, S.; Oikonomou, V. Integral $F(R)$ gravity and saddle point condition as a remedy for the H0-tension. *Nucl. Phys. B* **2022**, *980*, 115850. [CrossRef]
41. Spallicci, A.D.A.M.; Helayël-Neto, J.A.; López-Corredoira, M.; Capozziello, S. Cosmology and photon frequency shift induced by the Standard-Model Extension. *Eur. Phys. J. C* **2021**, *81*, 4. [CrossRef]
42. Spallicci, A.D.A.M.; Sarracino, G.; Capozziello, S. Investigating dark energy by electromagnetic frequency shifts. *Eur. Phys. J. Plus* **2022**, *137*, 253. [CrossRef]
43. Sarracino, G.; Spallicci, A.D.A.M.; Capozziello, S. Investigating dark energy by electromagnetic frequency shifts II: the Pantheon+ sample. *Eur. Phys. J. Plus* **2022**, *137*, 1386. [CrossRef]
44. Capozziello, S.; Benetti, M.; Spallicci, A.D.A.M. Addressing the cosmological H_0 tension by the Heisenberg uncertainty. *Found. Phys.* **2020**, *50*, 893. [CrossRef]
45. Spallicci, A.D.A.M.; Benetti, M.; Capozziello, S. Heisenberg principle at cosmological scales. *Found. Phys.* **2022**, *52*, 23. [CrossRef]
46. Bernal, J.L.; Verde, L.; Riess, A.G. The trouble with H_0. *J. Cosmol. Astropart. Phys.* **2016**, *2016*, 019. [CrossRef]
47. Mörtsell, E.; Dhawan, S. Does the Hubble constant tension call for new physics? *J. Cosmol. Astropart. Phys.* **2018**, *2018*, 025. [CrossRef]
48. Vagnozzi, S.; Dhawan, S.; Gerbino, M.; Freese, K.; Goobar, A.; Mena, O. Constraints on the sum of the neutrino masses in dynamical dark energy models with $w(z) \leq -1$ are tighter than those obtained in ΛCDM. *Phys. Rev. D* **2018**, *98*, 083501. [CrossRef]
49. Yang, W.; Pan, S.; Valentino, E.D.; Nunes, R.C.; Vagnozzi, S.; Mota, D.F. Tale of stable interacting dark energy, observational signatures, and the H_0 tension. *J. Cosmol. Astropart. Phys.* **2018**, *2018*, 019. [CrossRef]
50. Poulin, V.; Smith, T.L.; Karwal, T.; Kamionkowski, M. Early Dark Energy can Resolve the Hubble Tension. *Phys. Rev. Lett.* **2019**, *122*, 221301. [CrossRef]

51. Kreisch, C.D.; Cyr-Racine, F.Y.; Doré, O. Neutrino puzzle: Anomalies, interactions, and cosmological tensions. *Phys. Rev. D* **2020**, *101*, 103520. [CrossRef]
52. Agrawal, P.; Cyr-Racine, F.Y.; Pinner, D.; Randall, L. Rock 'n' Roll Solutions to the Hubble Tension. *Phys. Dark Universe* **2023**, *42*, 101347. [CrossRef]
53. Valentino, E.D.; Ferreira, R.Z.; Visinelli, L.; Danielsson, U. Late time transitions in the quintessence field and the H_0 tension. *Phys. Dark Universe* **2019**, *26*, 100385. [CrossRef]
54. Pan, S.; Yang, W.; Valentino, E.D.; Saridakis, E.N.; Chakraborty, S. Interacting scenarios with dynamical dark energy: Observational constraints and alleviation of the H_0 tension. *Phys. Rev. D* **2019**, *100*, 103520. [CrossRef]
55. Vagnozzi, S. New physics in light of the H_0 tension: An alternative view. *Phys. Rev. D* **2020**, *102*, 023518. [CrossRef]
56. Visinelli, L.; Vagnozzi, S.; Danielsson, U. Revisiting a Negative Cosmological Constant from Low-Redshift Data. *Symmetry* **2019**, *11*, 1035. [CrossRef]
57. Knox, L.; Millea, M. Hubble constant hunter's guide. *Phys. Rev. D* **2020**, *101*, 043533. [CrossRef]
58. Valentino, E.D.; Melchiorri, A.; Mena, O.; Vagnozzi, S. Interacting dark energy in the early 2020s: A promising solution to the H_0 and cosmic shear tensions. *Phys. Dark Universe* **2020**, *30*, 100666. [CrossRef]
59. Valentino, E.D.; Melchiorri, A.; Mena, O.; Vagnozzi, S. Non-minimal dark sector physics and cosmological tensions. *Phys. Rev. D* **2020**, *101*, 063502. [CrossRef]
60. Valentino, E.D.; Mukherjee, A.; Sen, A.A. Dark Energy with Phantom Crossing and the H_0 Tension. *Entropy* **2021**, *23*, 404. [CrossRef]
61. Smith, T.L.; Poulin, V.; Bernal, J.L.; Boddy, K.K.; Kamionkowski, M.; Murgia, R. Early dark energy is not excluded by current large-scale structure data. *Phys. Rev. D* **2021**, *103*, 123542. [CrossRef]
62. Vagnozzi, S. Consistency tests of ΛCDM from the early integrated Sachs-Wolfe effect: Implications for early-time new physics and the Hubble tension. *Phys. Rev. D* **2021**, *104*, 063524. [CrossRef]
63. Nunes, R.C.; Valentino, E.D. Dark sector interaction and the supernova absolute magnitude tension. *Phys. Rev. D* **2021**, *104*, 063529. [CrossRef]
64. Cyr-Racine, F.Y.; Ge, F.; Knox, L. Symmetry of Cosmological Observables, a Mirror World Dark Sector, and the Hubble Constant. *Phys. Rev. Lett.* **2022**, *128*, 201301. [CrossRef]
65. Anchordoqui, L.A.; Valentino, E.D.; Pan, S.; Yang, W. Dissecting the H0 and S8 tensions with Planck + BAO + supernova type Ia in multi-parameter cosmologies. *J. High Energy Astrophys.* **2021**, *32*, 28–64. [CrossRef]
66. Poulin, V.; Smith, T.L.; Bartlett, A. Dark energy at early times and ACT data: A larger Hubble constant without late-time priors. *Phys. Rev. D* **2021**, *104*, 123550. [CrossRef]
67. Alestas, G.; Camarena, D.; Valentino, E.D.; Kazantzidis, L.; Marra, V.; Nesseris, S.; Perivolaropoulos, L. Late-transition versus smooth $H(z)$ deformation models for the resolution of the Hubble crisis. *Phys. Rev. D* **2022**, *105*, 063538. [CrossRef]
68. Smith, T.L.; Lucca, M.; Poulin, V.; Abellan, G.F.; Balkenhol, L.; Benabed, K.; Galli, S.; Murgia, R. Hints of early dark energy in Planck , SPT, and ACT data: New physics or systematics? *Phys. Rev. D* **2022**, *106*, 043526. [CrossRef]
69. Reeves, A.; Herold, L.; Vagnozzi, S.; Sherwin, B.D.; Ferreira, E.G.M. Restoring cosmological concordance with early dark energy and massive neutrinos? *Mon. Not. R. Astron. Soc.* **2023**, *520*, 3688–3695. [CrossRef]
70. Poulin, V.; Smith, T.L.; Karwal, T. The Ups and Downs of Early Dark Energy solutions to the Hubble tension: A review of models, hints and constraints circa 2023. *arXiv* **2023**, arXiv:2302.09032.
71. Demianski, M.; Piedipalumbo, E.; Sawant, D.; Amati, L. Cosmology with gamma-ray bursts I. The Hubble diagram through the calibrated $E_{p,i} - E_{iso}$ correlation. *Astron. Astrophys.* **2017**, *598*, A112. [CrossRef]
72. Lusso, E.; Piedipalumbo, E.; Risaliti, G.; Paolillo, M.; Bisogni, S.; Nardini, E.; Amati, L. Tension with the flat ΛCDM model from a high-redshift Hubble diagram of supernovae, quasars, and gamma-ray bursts. *Astron. Astrophys.* **2019**, *628*, L4. [CrossRef]
73. Ryan, J.; Chen, Y.; Ratra, B. Baryon acoustic oscillation, Hubble parameter, and angular size measurement constraints on the Hubble constant, dark energy dynamics, and spatial curvature. *Mon. Not. R. Astron. Soc.* **2019**, *488*, 3844–3856. [CrossRef]
74. Cao, S.; Ryan, J.; Ratra, B. Using Pantheon and DES supernova, baryon acoustic oscillation, and Hubble parameter data to constrain the Hubble constant, dark energy dynamics, and spatial curvature. *Mon. Not. R. Astron. Soc.* **2021**, *504*, 300–310. [CrossRef]
75. Krishnan, C.; Colgáin, E.Ó.; Sheikh-Jabbari, M.; Yang, T. Running Hubble tension and a H0 diagnostic. *Phys. Rev. D* **2021**, *103*, 103509. [CrossRef]
76. Colgáin, E.Ó.; Sheikh-Jabbari, M.; Yang, T. Elucidating cosmological model dependence with H_0. *Eur. Phys. J. C* **2021**, *81*, 892. [CrossRef]
77. Krishnan, C.; Mondol, R. H_0 as a Universal FLRW Diagnostic. *arXiv* **2022**, arXiv:2201.13384.
78. Colgáin, E.Ó.; Sheikh-Jabbari, M.; Solomon, R.; Bargiacchi, G.; Capozziello, S.; Dainotti, M.; Stojkovic, D. Revealing intrinsic flat ΛCDM biases with standardizable candles. *Phys. Rev. D* **2022**, *106*, L041301. [CrossRef]
79. Colgáin, E.Ó.; Sheikh-Jabbari, M.M.; Solomon, R.; Dainotti, M.G.; Stojkovic, D. Putting Flat ΛCDM In The (Redshift) Bin. *arXiv* **2022**, arXiv:2206.11447.
80. Colgáin, E.Ó.; Sheikh-Jabbari, M.M.; Solomon, R. High Redshift ΛCDM Cosmology: To Bin or not to Bin? *arXiv* **2022**, arXiv:2211.02129.

81. Dainotti, M.G.; Simone, B.D.; Schiavone, T.; Montani, G.; Rinaldi, E.; Lambiase, G. On the Hubble Constant Tension in the SNe Ia Pantheon Sample. *Astrophys. J.* **2021**, *912*, 150. [CrossRef]
82. Dainotti, M.G.; Simone, B.D.; Schiavone, T.; Montani, G.; Rinaldi, E.; Lambiase, G.; Bogdan, M.; Ugale, S. On the Evolution of the Hubble Constant with the SNe Ia Pantheon Sample and Baryon Acoustic Oscillations: A Feasibility Study for GRB-Cosmology in 2030. *Galaxies* **2022**, *10*, 24. [CrossRef]
83. Dainotti, M.; De Simone, B.; Montani, G.; Schiavone, T.; Lambiase, G. The Hubble constant tension: Current status and future perspectives through new cosmological probes. *arXiv* **2023**, arXiv:2301.10572.
84. Schiavone, T.; Montani, G.; Dainotti, M.G.; De Simone, B.; Rinaldi, E.; Lambiase, G. Running Hubble constant from the SNe Ia Pantheon sample? *arXiv* **2022**, arXiv:2205.07033.
85. Schiavone, T.; Montani, G.; Bombacigno, F. $f(R)$ gravity in the Jordan frame as a paradigm for the Hubble tension. *Mon. Not. R. Astron. Soc. Lett.* **2023**, *522*, L72–L77. [CrossRef]
86. Malekjani, M.; Conville, R.M.; Colgáin, E.Ó.; Pourojaghi, S.; Sheikh-Jabbari, M.M. Negative Dark Energy Density from High Redshift Pantheon+ Supernovae. *arXiv* **2023**, arXiv:2301.12725. https://doi.org/10.48550/ARXIV.2301.12725.
87. Gurzadyan, V.G.; Fimin, N.N.; Chechetkin, V.M. Cosmic voids and the kinetic analysis. *Astron. Astrophys.* **2022**, *666*, A149. [CrossRef]
88. Hu, J.P.; Wang, F.Y. Hubble Tension: The Evidence of New Physics. *Universe* **2023**, *9*, 94. [CrossRef]
89. Jia, X.A.; Hu, J.P.; Wang, F.Y. Evidence of a decreasing trend for the Hubble constant. *Astron. Astrophys.* **2023**, *674*, A45. [CrossRef]
90. Capozziello, S.; Sarracino, G.; Spallicci, A.D.A.M. Questioning the H_0 tension via the look-back time. *Phys. Dark Universe* **2023**, *40*, 101201. [CrossRef]
91. Mecke, K.R.; Buchert, T.; Wagner, H. Robust morphological measures for large-scale structure in the Universe. *Astron. Astrophys.* **1994**, *288*, 697–704. [CrossRef]
92. Yadav, J.K.; Bagla, J.S.; Khandai, N. Fractal dimension as a measure of the scale of homogeneity. *Mon. Not. R. Astron. Soc.* **2010**, *405*, 2009–2015. [CrossRef]
93. Wiegand, A.; Buchert, T.; Ostermann, M. Direct Minkowski Functional analysis of large redshift surveys: A new high-speed code tested on the luminous red galaxy Sloan Digital Sky Survey-DR7 catalogue. *Mon. Not. R. Astron. Soc.* **2014**, *443*, 241–259. [CrossRef]
94. Robertson, H.P. Kinematics and World-Structure. *Astrophys. J.* **1935**, *82*, 284. [CrossRef]
95. Friedmann, A. Uber die Krummung des Raumes. *Z. Fur Phys.* **1922**, *10*, 377–386. [CrossRef]
96. Hogg, D.W. Distance measures in cosmology. *arXiv* **1999**, arXiv:astro-ph/9905116.
97. Nemiroff, R.J.; Patla, B. Adventures in Friedmann cosmology: A detailed expansion of the cosmological Friedmann equations. *Am. J. Phys.* **2008**, *76*, 265–276. [CrossRef]
98. Riess, A.G.; Casertano, S.; Yuan, W.; Bowers, J.B.; Macri, L.; Zinn, J.C.; Scolnic, D. Cosmic Distances Calibrated to 1% Precision with Gaia EDR3 Parallaxes and Hubble Space Telescope Photometry of 75 Milky Way Cepheids Confirm Tension with ΛCDM. *Astrophys. J. Lett.* **2021**, *908*, L6. [CrossRef]
99. Pietrzyński, G.; Graczyk, D.; Gallenne, A.; Gieren, W.; Thompson, I.B.; Pilecki, B.; Karczmarek, P.; Górski, M.; Suchomska, K.; Taormina, M.; et al. A distance to the Large Magellanic Cloud that is precise to one per cent. *Nature* **2019**, *567*, 200–203. [CrossRef]
100. Reid, M.J.; Pesce, D.W.; Riess, A.G. An Improved Distance to NGC 4258 and Its Implications for the Hubble Constant. *Astrophys. J.* **2019**, *886*, L27. [CrossRef]
101. Riess, A.G.; Casertano, S.; Yuan, W.; Macri, L.M.; Scolnic, D. Large Magellanic Cloud Cepheid Standards Provide a 1% Foundation for the Determination of the Hubble Constant and Stronger Evidence for Physics beyond ΛCDM. *Astrophys. J.* **2019**, *876*, 85. [CrossRef]
102. Gaia Collaboration; Prusti, T.; de Bruijne, J.H.J.; Brown, A.G.A.; Vallenari, A.; Babusiaux, C.; Bailer-Jones, C.A.L.; Bastian, U.; Biermann, M.; Evans, D.W.; et al. The Gaia mission. *Astron. Astrophys.* **2016**, *595*, A1. [CrossRef]
103. Gaia Collaboration; Brown, A.G.A.; Vallenari, A.; Prusti, T.; de Bruijne, J.H.J.; Mignard, F.; Drimmel, R.; Babusiaux, C.; Bailer-Jones, C.A.L.; Bastian, U.; et al. Gaia Data Release 1. Summary of the astrometric, photometric, and survey properties. *Astron. Astrophys.* **2016**, *595*, A2. [CrossRef]
104. Gaia Collaboration; Brown, A.G.A.; Vallenari, A.; Prusti, T.; de Bruijne, J.H.J.; Babusiaux, C.; Bailer-Jones, C.A.L.; Biermann, M.; Evans, D.W.; Eyer, L.; et al. Gaia Data Release 2. Summary of the contents and survey properties. *Astron. Astrophys.* **2018**, *616*, A1. [CrossRef]
105. Brown, A.G.A.; Vallenari, A.; Prusti, T.; de Bruijne, J.H.J.; Babusiaux, C.; Biermann, M.; Creevey, O.L.; Evans, D.W.; Eyer, L.; Hutton, A.; et al. Gaia Early Data Release 3. *Astron. Astrophys.* **2021**, *650*, C3. [CrossRef]
106. Ripepi, V.; Clementini, G.; Molinaro, R.; Leccia, S.; Plachy, E.; Molnár, L.; Rimoldini, L.; Musella, I.; Marconi, M.; Garofalo, A.; et al. Gaia Data Release 3. Specific processing and validation of all sky RR Lyrae and Cepheid stars: The Cepheid sample. *Astron. Astrophys.* **2023**, *674*, A17. [CrossRef]
107. Marconi, M.; Molinaro, R.; Bono, G.; Pietrzy'nski, G.; Gieren, W.; Pilecki, B.; Stellingwerf, R.F.; Graczyk, D.; Smolec, R.; Konorski, P.; et al. The Eclipsing Binary Cepheid OGLE-LMC-CEP-0227 in the Large Magellanic Cloud: Pulsation modelling of light and radial velocity curves. *Astrophys. J.* **2013**, *768*, L6. [CrossRef]
108. Somma, G.D.; Marconi, M.; Molinaro, R.; Cignoni, M.; Musella, I.; Ripepi, V. An Extended Theoretical Scenario for Classical Cepheids. I. Modeling Galactic Cepheids in the Gaia Photometric System. *Astrophys. J. Suppl. Ser.* **2020**, *247*, 30. [CrossRef]

109. De Somma, G.; Marconi, M.; Molinaro, R.; Cignoni, M.; Musella, I.; Ripepi, V. Gaia Parallaxes Versus Updated Pulsation Model Predictions. In *Proceedings of the RR Lyrae/Cepheid 2019: Frontiers of Classical Pulsators*; Astronomical Society of the Pacific Conference Series; Kinemuchi, K., Lovekin, C., Neilson, H., Vivas, K., Eds.; Astronomical Society of the Pacific: San Francisco, CA, USA, 2021; Volume 529, p. 27.
110. Marconi, M.; Musella, I.; Fiorentino, G. Cepheid Pulsation Models at Varying Metallicity and $\Delta Y/\Delta Z$. *Astrophys. J.* **2005**, *632*, 590–610. [CrossRef]
111. Ripepi, V.; Catanzaro, G.; Molinaro, R.; Gatto, M.; De Somma, G.; Marconi, M.; Romaniello, M.; Leccia, S.; Musella, I.; Trentin, E.; et al. Cepheid metallicity in the Leavitt law (C-metall) survey—I. HARPS-N@TNG spectroscopy of 47 classical Cepheids and 1 BL Her variables. *Mon. Not. R. Astron. Soc.* **2021**, *508*, 4047–4071. [CrossRef]
112. De Somma, G.; Marconi, M.; Molinaro, R.; Ripepi, V.; Leccia, S.; Musella, I. An Updated Metal-dependent Theoretical Scenario for Classical Cepheids. *Astrophys. J. Suppl. Ser.* **2022**, *262*, 25. [CrossRef]
113. Breuval, L.; Riess, A.G.; Kervella, P.; Anderson, R.I.; Romaniello, M. An Improved Calibration of the Wavelength Dependence of Metallicity on the Cepheid Leavitt Law. *Astrophys. J.* **2022**, *939*, 89. [CrossRef]
114. Meng, X.; Gao, Y.; Han, Z. SNe Ia as a cosmological probe. *Int. J. Mod. Phys. D* **2015**, *24*, 1530029. [CrossRef]
115. Scolnic, D.; Brout, D.; Carr, A.; Riess, A.G.; Davis, T.M.; Dwomoh, A.; Jones, D.O.; Ali, N.; Charvu, P.; Chen, R.; et al. The Pantheon+ Analysis: The Full Data Set and Light-curve Release. *Astrophys. J.* **2022**, *938*, 113. [CrossRef]
116. Brout, D.; Scolnic, D.; Popovic, B.; Riess, A.G.; Carr, A.; Zuntz, J.; Kessler, R.; Davis, T.M.; Hinton, S.; Jones, D.; et al. The Pantheon+ Analysis: Cosmological Constraints. *Astrophys. J.* **2022**, *938*, 110. [CrossRef]
117. Scolnic, D.M.; Jones, D.O.; Rest, A.; Pan, Y.C.; Chornock, R.; Foley, R.J.; Huber, M.E.; Kessler, R.; Narayan, G.; Riess, A.G.; et al. The complete light-curve sample of spectroscopically confirmed SNe Ia from Pan-STARRS1 and cosmological constraints from the combined Pantheon sample. *Astrophys. J.* **2018**, *859*, 101. [CrossRef]
118. Hillebrandt, W.; Niemeyer, J.C. Type Ia Supernova Explosion Models. *Annu. Rev. Astron. Astrophys.* **2000**, *38*, 191–230. [CrossRef]
119. Nomoto, K.; Thielemann, F.K.; Yokoi, K. Accreting white dwarf models for type I supern. III. Carbon deflagration supernovae. *Astrophys. J.* **1984**, *286*, 644–658. [CrossRef]
120. Colgate, S.A.; McKee, C. Early Supernova Luminosity. *Astrophys. J.* **1969**, *157*, 623. [CrossRef]
121. Carroll, S.M. The Cosmological Constant. *Living Rev. Relativ.* **2001**, *4*, 1. [CrossRef]
122. Filippenko, A.V.; Richmond, M.W.; Matheson, T.; Shields, J.C.; Burbidge, E.M.; Cohen, R.D.; Dickinson, M.; Malkan, M.A.; Nelson, B.; Pietz, J.; et al. The Peculiar Type IA SN 1991T: Detonation of a White Dwarf? *Astrophys. J. Lett.* **1992**, *384*, L15. [CrossRef]
123. Filippenko, A.V.; Richmond, M.W.; Branch, D.; Gaskell, M.; Herbst, W.; Ford, C.H.; Treffers, R.R.; Matheson, T.; Ho, L.C.; Dey, A.; et al. The Subluminous, Spectroscopically Peculiar Type 1a Supernova 1991bg in the Elliptical Galaxy NGC 4374. *Astrophys. J.* **1992**, *104*, 1543. [CrossRef]
124. Khokhlov, A.M. Delayed detonation model for type IA supernovae. *Astron. Astrophys.* **1991**, *245*, 114–128.
125. Phillips, M.M. The Absolute Magnitudes of Type IA Supernovae. *Astrophys. J. Lett.* **1993**, *413*, L105. [CrossRef]
126. Salaris, M.; Cassisi, S. The "tip" of the red giant branch as a distance indicator: Results from evolutionary models. *Mon. Not. R. Astron. Soc.* **1997**, *289*, 406–414. [CrossRef]
127. Freedman, W.L.; Madore, B.F.; Hatt, D.; Hoyt, T.J.; Jang, I.S.; Beaton, R.L.; Burns, C.R.; Lee, M.G.; Monson, A.J.; Neeley, J.R.; et al. The Carnegie-Chicago Hubble Program. VIII. An Independent Determination of the Hubble Constant Based on the Tip of the Red Giant Branch. *Astrophys. J.* **2019**, *882*, 34. [CrossRef]
128. de Jaeger, T.; Stahl, B.E.; Zheng, W.; Filippenko, A.V.; Riess, A.G.; Galbany, L. A measurement of the Hubble constant from Type II supernovae. *Mon. Not. R. Astron. Soc.* **2020**, *496*, 3402–3411. [CrossRef]
129. Kourkchi, E.; Tully, R.B.; Anand, G.S.; Courtois, H.M.; Dupuy, A.; Neill, J.D.; Rizzi, L.; Seibert, M. Cosmicflows-4: The Calibration of Optical and Infrared Tully-Fisher Relations. *Astrophys. J.* **2020**, *896*, 3. [CrossRef]
130. Blakeslee, J.P.; Jensen, J.B.; Ma, C.P.; Milne, P.A.; Greene, J.E. The Hubble Constant from Infrared Surface Brightness Fluctuation Distances. *Astrophys. J.* **2021**, *911*, 65. [CrossRef]
131. Uddin, S.A.; Burns, C.R.; Phillips, M.M.; Suntzeff, N.B.; Freedman, W.L.; Brown, P.J.; Morrell, N.; Hamuy, M.; Krisciunas, K.; Wang, L.; et al. Carnegie Supernova Project-I and -II: Measurements of H_0 using Cepheid, TRGB, and SBF Distance Calibration to Type Ia Supernovae. *arXiv* **2023**, arXiv:2308.01875.
132. Cardona, W.; Kunz, M.; Pettorino, V. Determining H_0 with Bayesian hyper-parameters. *J. Cosmol. Astropart. Phys.* **2017**, *2017*, 056. [CrossRef]
133. Camarena, D.; Marra, V. Local determination of the Hubble constant and the deceleration parameter. *Phys. Rev. Res.* **2020**, *2*. [CrossRef]
134. Dhawan, S.; Jha, S.W.; Leibundgut, B. Measuring the Hubble constant with Type Ia supernovae as near-infrared standard candles. *Astron. Astrophys.* **2018**, *609*, A72. [CrossRef]
135. Burns, C.R.; Parent, E.; Phillips, M.M.; Stritzinger, M.; Krisciunas, K.; Suntzeff, N.B.; Hsiao, E.Y.; Contreras, C.; Anais, J.; Boldt, L.; et al. The Carnegie Supernova Project: Absolute Calibration and the Hubble Constant. *Astrophys. J.* **2018**, *869*, 56. [CrossRef]
136. Follin, B.; Knox, L. Insensitivity of the distance ladder Hubble constant determination to Cepheid calibration modelling choices. *Mon. Not. R. Astron. Soc.* **2018**, *477*, 4534–4542. [CrossRef]
137. Feeney, S.M.; Mortlock, D.J.; Dalmasso, N. Clarifying the Hubble constant tension with a Bayesian hierarchical model of the local distance ladder. *Mon. Not. R. Astron. Soc.* **2018**, *476*, 3861–3882. [CrossRef]

138. Freedman, W.L.; Madore, B.F.; Hoyt, T.; Jang, I.S.; Beaton, R.; Lee, M.G.; Monson, A.; Neeley, J.; Rich, J. Calibration of the Tip of the Red Giant Branch. *Astrophys. J.* **2020**, *891*, 57. [CrossRef]
139. Freedman, W.L. Measurements of the Hubble Constant: Tensions in Perspective. *Astrophys. J.* **2021**, *919*, 16. [CrossRef]
140. Jang, I.S.; Lee, M.G. The Tip of the Red Giant Branch Distances to Typa Ia Supernova Host Galaxies. V. NGC 3021, NGC 3370, and NGC 1309 and the Value of the Hubble Constant. *Astrophys. J.* **2017**, *836*, 74. [CrossRef]
141. Yuan, W.; Riess, A.G.; Macri, L.M.; Casertano, S.; Scolnic, D.M. Consistent Calibration of the Tip of the Red Giant Branch in the Large Magellanic Cloud on the Hubble Space Telescope Photometric System and a Redetermination of the Hubble Constant. *Astrophys. J.* **2019**, *886*, 61. [CrossRef]
142. Kim, Y.J.; Kang, J.; Lee, M.G.; Jang, I.S. Determination of the Local Hubble Constant from Virgo Infall Using TRGB Distances. *Astrophys. J.* **2020**, *905*, 104. [CrossRef]
143. Jones, D.O.; Mandel, K.S.; Kirshner, R.P.; Thorp, S.; Challis, P.M.; Avelino, A.; Brout, D.; Burns, C.; Foley, R.J.; Pan, Y.C.; et al. Cosmological Results from the RAISIN Survey: Using Type Ia Supernovae in the Near Infrared as a Novel Path to Measure the Dark Energy Equation of State. *Astrophys. J.* **2022**, *933*, 172. [CrossRef]
144. Dhawan, S.; Goobar, A.; Johansson, J.; Jang, I.S.; Rigault, M.; Harvey, L.; Maguire, K.; Freedman, W.L.; Madore, B.F.; Smith, M.; et al. A Uniform Type Ia Supernova Distance Ladder with the Zwicky Transient Facility: Absolute Calibration Based on the Tip of the Red Giant Branch Method. *Astrophys. J.* **2022**, *934*, 185. [CrossRef]
145. Scolnic, D.; Riess, A.G.; Wu, J.; Li, S.; Anand, G.S.; Beaton, R.; Casertano, S.; Anderson, R.; Dhawan, S.; Ke, X. CATS: The Hubble Constant from Standardized TRGB and Type Ia Supernova Measurements. *Astrophys. J. Lett.* **2023**, *954*, L31. [CrossRef]
146. Khetan, N.; Izzo, L.; Branchesi, M.; Wojtak, R.; Cantiello, M.; Murugeshan, C.; Agnello, A.; Cappellaro, E.; Valle, M.D.; Gall, C.; et al. A new measurement of the Hubble constant using Type Ia supernovae calibrated with surface brightness fluctuations. *Astron. Astrophys.* **2021**, *647*, A72. [CrossRef]
147. Cantiello, M.; Jensen, J.B.; Blakeslee, J.P.; Berger, E.; Levan, A.J.; Tanvir, N.R.; Raimondo, G.; Brocato, E.; Alexander, K.D.; Blanchard, P.K.; et al. A Precise Distance to the Host Galaxy of the Binary Neutron Star Merger GW170817 Using Surface Brightness Fluctuations. *Astrophys. J.* **2018**, *854*, L31. [CrossRef]
148. de Jaeger, T.; Galbany, L.; Riess, A.G.; Stahl, B.E.; Shappee, B.J.; Filippenko, A.V.; Zheng, W. A 5% measurement of the Hubble-Lemaître constant from Type II supernovae. *Mon. Not. R. Astron. Soc.* **2022**, *514*, 4620–4628. [CrossRef]
149. Schombert, J.; McGaugh, S.; Lelli, F. Using the Baryonic Tully-Fisher Relation to Measure H_0. *Astron. J.* **2020**, *160*, 71. [CrossRef]
150. Kourkchi, E.; Tully, R.B.; Courtois, H.M.; Dupuy, A.; Guinet, D. Cosmicflows-4: The baryonic Tully-Fisher relation providing ∼10000 distances. *Mon. Not. R. Astron. Soc.* **2022**, *511*, 6160–6178. [CrossRef]
151. Bonvin, V.; Courbin, F.; Suyu, S.H.; Marshall, P.J.; Rusu, C.E.; Sluse, D.; Tewes, M.; Wong, K.C.; Collett, T.; Fassnacht, C.D.; et al. H0LiCOW V. New COSMOGRAIL time delays of HE 0435-1223: H_0 to 3.8% precision from strong lensing in a flat ΛCDM model. *Mon. Not. R. Astron. Soc.* **2016**, *465*, 4914–4930. [CrossRef]
152. Birrer, S.; Treu, T.; Rusu, C.E.; Bonvin, V.; Fassnacht, C.D.; Chan, J.H.H.; Agnello, A.; Shajib, A.J.; Chen, G.C.F.; Auger, M.; et al. H0LiCOW IX. Cosmographic analysis of the doubly imaged quasar SDSS 1206+332 and a new measurement of the Hubble constant. *Mon. Not. R. Astron. Soc.* **2019**, *484*, 4726–4753. [CrossRef]
153. Wong, K.C.; Suyu, S.H.; Chen, G.C.F.; Rusu, C.E.; Millon, M.; Sluse, D.; Bonvin, V.; Fassnacht, C.D.; Taubenberger, S.; Auger, M.W.; et al. H0LiCOW-XIII. A 2.4 per cent measurement of H0 from lensed quasars: 5.3σ tension between early- and late-Universe probes. *Mon. Not. R. Astron. Soc.* **2019**, *498*, 1420–1439. [CrossRef]
154. Millon, M.; Galan, A.; Courbin, F.; Treu, T.; Suyu, S.H.; Ding, X.; Birrer, S.; Chen, G.C.F.; Shajib, A.J.; Sluse, D.; et al. TDCOSMO. *Astron. Astrophys.* **2020**, *639*, A101. [CrossRef]
155. Krishnan, C.; Mohayaee, R.; Colgáin, E.Ó.; Sheikh-Jabbari, M.M.; Yin, L. Does Hubble tension signal a breakdown in FLRW cosmology? *Class. Quantum Gravity* **2021**, *38*, 184001. [CrossRef]
156. Verde, L.; Treu, T.; Riess, A.G. Tensions between the early and late Universe. *Nat. Astron.* **2019**, *3*, 891–895. [CrossRef]
157. Di Valentino, E. A combined analysis of the H_0 late time direct measurements and the impact on the Dark Energy sector. *Mon. Not. R. Astron. Soc.* **2021**, *502*, 2065–2073. [CrossRef]
158. Hinshaw, G.; Larson, D.; Komatsu, E.; Spergel, D.N.; Bennett, C.L.; Dunkley, J.; Nolta, M.R.; Halpern, M.; Hill, R.S.; Odegard, N.; et al. Nine-Year Wilkinson Microwave Anisotropy Probe (WMAP) Observations: Cosmological Parameter Results. *Astrophys. J. Suppl. Ser.* **2013**, *208*, 19. [CrossRef]
159. Aiola, S.; Calabrese, E.; Maurin, L.; Naess, S.; Schmitt, B.L.; Abitbol, M.H.; Addison, G.E.; Ade, P.A.R.; Alonso, D.; Amiri, M.; et al. The Atacama Cosmology Telescope: DR4 maps and cosmological parameters. *J. Cosmol. Astropart. Phys.* **2020**, *2020*, 047. [CrossRef]
160. Dutcher, D.; Balkenhol, L.; Ade, P.; Ahmed, Z.; Anderes, E.; Anderson, A.; Archipley, M.; Avva, J.; Aylor, K.; Barry, P.; et al. Measurements of the E-Mode Polarization and Temperature-E-Mode Correlation of the CMB from SPT-3G 2018 Data. *Phys. Rev. D* **2021**, *104*, 022003. [CrossRef]
161. Eisenstein, D.J.; Zehavi, I.; Hogg, D.W.; Scoccimarro, R.; Blanton, M.R.; Nichol, R.C.; Scranton, R.; Seo, H.; Tegmark, M.; Zheng, Z.; et al. Detection of the Baryon Acoustic Peak in the Large-Scale Correlation Function of SDSS Luminous Red Galaxies. *Astrophys. J.* **2005**, *633*, 560–574. [CrossRef]

162. Beutler, F.; Blake, C.; Colless, M.; Jones, D.H.; Staveley-Smith, L.; Campbell, L.; Parker, Q.; Saunders, W.; Watson, F. The 6dF Galaxy Survey: Baryon acoustic oscillations and the local Hubble constant. *Mon. Not. R. Astron. Soc.* **2011**, *416*, 3017–3032. [CrossRef]
163. Blake, C.; Brough, S.; Colless, M.; Contreras, C.; Couch, W.; Croom, S.; Croton, D.; Davis, T.M.; Drinkwater, M.J.; Forster, K.; et al. The WiggleZ Dark Energy Survey: Joint measurements of the expansion and growth history at $z < 1$. *Mon. Not. R. Astron. Soc.* **2012**, *425*, 405–414. [CrossRef]
164. du Mas des Bourboux, H.; Rich, J.; Font-Ribera, A.; de Sainte Agathe, V.; Farr, J.; Etourneau, T.; Goff, J.M.L.; Cuceu, A.; Balland, C.; Bautista, J.E.; et al. The Completed SDSS-IV Extended Baryon Oscillation Spectroscopic Survey: Baryon Acoustic Oscillations with Lyα Forests. *Astrophys. J.* **2020**, *901*, 153. [CrossRef]
165. Alam, S.; Aubert, M.; Avila, S.; Balland, C.; Bautista, J.E.; Bershady, M.A.; Bizyaev, D.; Blanton, M.R.; Bovy, A.S.B.J.; Brinkmann, J.; et al. Completed SDSS-IV extended Baryon Oscillation Spectroscopic Survey: Cosmological implications from two decades of spectroscopic surveys at the Apache Point Observatory. *Phys. Rev. D* **2021**, *103*, 083553. [CrossRef]
166. Cooke, R.J.; Pettini, M.; Steidel, C.C. One Percent Determination of the Primordial Deuterium Abundance. *Astrophys. J.* **2018**, *855*, 102. [CrossRef]
167. Ivanov, M.M.; Simonović , M.; Zaldarriaga, M. Cosmological parameters from the BOSS galaxy power spectrum. *J. Cosmol. Astropart. Phys.* **2020**, *2020*, 042. [CrossRef]
168. d'Amico, G.; Gleyzes, J.; Kokron, N.; Markovic, K.; Senatore, L.; Zhang, P.; Beutler, F.; Gil-Marín, H. The cosmological analysis of the SDSS/BOSS data from the Effective Field Theory of Large-Scale Structure. *J. Cosmol. Astropart. Phys.* **2020**, *2020*, 005. [CrossRef]
169. Philcox, O.H.; Ivanov, M.M.; Simonović , M.; Zaldarriaga, M. Combining full-shape and BAO analyses of galaxy power spectra: A 1.6% CMB-independent constraint on H_0. *J. Cosmol. Astropart. Phys.* **2020**, *2020*, 032. [CrossRef]
170. Ivanov, M.M. Cosmological constraints from the power spectrum of eBOSS emission line galaxies. *Phys. Rev. D* **2021**, *104*, 103514. [CrossRef]
171. Ivanov, M.M.; Philcox, O.H.; Simonović, M.; Zaldarriaga, M.; Nischimichi, T.; Takada, M. Cosmological constraints without nonlinear redshift-space distortions. *Phys. Rev. D* **2022**, *105*, 043531. [CrossRef]
172. Philcox, O.H.; Ivanov, M.M. The BOSS DR12 Full-Shape Cosmology: Λ CDM Constraints from the Large-Scale Galaxy Power Spectrum and Bispectrum Monopole. *Phys. Rev. D* **2022**, *105*, 043517. [CrossRef]
173. Chen, S.F.; Vlah, Z.; White, M. A new analysis of galaxy 2-point functions in the BOSS survey, including full-shape information and post-reconstruction BAO. *J. Cosmol. Astropart. Phys.* **2022**, *2022*, 008. [CrossRef]
174. Brieden, S.; Gil-Marín, H.; Verde, L. Model-independent versus model-dependent interpretation of the SDSS-III BOSS power spectrum: Bridging the divide. *Phys. Rev. D* **2021**, *104*, L121301. [CrossRef]
175. Dainotti, M.G.; Sarracino, G.; Capozziello, S. Gamma-ray bursts, supernovae Ia, and baryon acoustic oscillations: A binned cosmological analysis. *Publ. Astron. Soc. Jpn.* **2022**, *74*, 1095–1113. [CrossRef]
176. Bond, J.R.; Efstathiou, G. The statistics of cosmic background radiation fluctuations. *Mon. Not. R. Astron. Soc.* **1987**, *226*, 655–687. [CrossRef]
177. Eisenstein, D.J.; Hu, W. Baryonic Features in the Matter Transfer Function. *Astrophys. J.* **1998**, *496*, 605–614. [CrossRef]
178. Bashinsky, S.; Bertschinger, E. Position-Space Description of the Cosmic Microwave Background and Its Temperature Correlation Function. *Phys. Rev. Lett.* **2001**, *87*, 081301. [CrossRef] [PubMed]
179. Bassett, B.A.; Hlozek, R. Baryon Acoustic Oscillations. *arXiv* **2009**, arXiv:0910.5224.
180. Dawson, K.S.; Schlegel, D.J.; Ahn, C.P.; Anderson, S.F.; Aubourg, É.; Bailey, S.; Barkhouser, R.H.; Bautista, J.E.; Beifiori, A.; Berlind, A.A.; et al. The Baryon Oscillation Spectroscopic Survey of SDSS-III. *Astron. J.* **2013**, *145*, 10. [CrossRef]
181. Eisenstein, D.J.; Weinberg, D.H.; Agol, E.; Aihara, H.; Prieto, C.A.; Anderson, S.F.; Arns, J.A.; Aubourg, É.; Bailey, S.; Balbinot, E.; et al. SDSS-III: Massive Spectroscopic Surveys of the Distant Universe, the Milky Way Galaxy, and Extra-Solar Planetary Systems. *Astron. J.* **2011**, *142*, 72. [CrossRef]
182. Dawson, K.S.; Kneib, J.P.; Percival, W.J.; Alam, S.; Albareti, F.D.; Anderson, S.F.; Armengaud, E.; Aubourg, É.; Bailey, S.; Bautista, J.E.; et al. The SDSS-IV extended Baryon Oscillation Spectroscopic Survey: Overview and Early Data. *Astron. J.* **2016**, *151*, 44. [CrossRef]
183. Blanton, M.R.; Bershady, M.A.; Abolfathi, B.; Albareti, F.D.; Allende Prieto, C.; Almeida, A.; Alonso-García, J.; Anders, F.; Anderson, S.F.; Andrews, B.; et al. Sloan Digital Sky Survey IV: Mapping the Milky Way, Nearby Galaxies, and the Distant Universe. *Astrophys. J.* **2017**, *154*, 28. [CrossRef]
184. Ross, A.J.; Samushia, L.; Howlett, C.; Percival, W.J.; Burden, A.; Manera, M. The clustering of the SDSS DR7 main Galaxy sample—I. A 4 per cent distance measure at $z = 0.15$. *Mon. Not. R. Astron. Soc.* **2015**, *449*, 835–847. [CrossRef]
185. Aubourg, E.; Bailey, S.; Bautista, J.E.; Beutler, F.; Bhardwaj, V.; Bizyaev, D.; Blanton, M.; Blomqvist, M.; Bolton, A.S.; Bovy, J.; et al. Cosmological implications of baryon acoustic oscillation measurements. *Phys. Rev. D* **2015**, *92*, 123516. [CrossRef]
186. Abbott, B.P.; Abbott, R.; Abbott, T.; Acernese, F.; Ackley, K.; Adams, C.; Adams, T.; Addesso, P.; Adhikari, R.; Adya, V.; et al. GW170817: Observation of Gravitational Waves from a Binary Neutron Star Inspiral. *Phys. Rev. Lett.* **2017**, *119*, 161101. [CrossRef] [PubMed]

187. Guidorzi, C.; Margutti, R.; Brout, D.; Scolnic, D.; Fong, W.; Alexander, K.D.; Cowperthwaite, P.S.; Annis, J.; Berger, E.; Blanchard, P.K.; et al. Improved Constraints on H_0 from a Combined Analysis of Gravitational-wave and Electromagnetic Emission from GW170817. *Astrophys. J.* **2017**, *851*, L36. [CrossRef]
188. Soares-Santos, M.; Palmese, A.; Hartley, W.; Annis, J.; Garcia-Bellido, J.; Lahav, O.; Doctor, Z.; Fishbach, M.; Holz, D.E.; Lin, H.; et al. First Measurement of the Hubble Constant from a Dark Standard Siren using the Dark Energy Survey Galaxies and the LIGO/Virgo Binary-Black-hole Merger GW170814. *Astrophys. J.* **2019**, *876*, L7. [CrossRef]
189. Gayathri, V.; Healy, J.; Lange, J.; O'Brien, B.; Szczepanczyk, M.; Bartos, I.; Campanelli, M.; Klimenko, S.; Lousto, C.; O'Shaughnessy, R. Hubble Constant Measurement with GW190521 as an Eccentric Black Hole Merger. *arXiv* **2020**, arXiv:2009.14247.
190. Palmese, A.; Bom, C.R.; Mucesh, S.; Hartley, W.G. A Standard Siren Measurement of the Hubble Constant Using Gravitational-wave Events from the First Three LIGO/Virgo Observing Runs and the DESI Legacy Survey. *Astrophys. J.* **2023**, *943*, 56. [CrossRef]
191. Jimenez, R.; Cimatti, A.; Verde, L.; Moresco, M.; Wandelt, B. The local and distant Universe: Stellar ages and H_0. *J. Cosmol. Astropart. Phys.* **2019**, *2019*, 043. [CrossRef]
192. Bernal, J.L.; Verde, L.; Jimenez, R.; Kamionkowski, M.; Valcin, D.; Wandelt, B.D. Trouble beyond H_0 and the new cosmic triangles. *Phys. Rev. D* **2021**, *103*, 103533. [CrossRef]
193. Boylan-Kolchin, M.; Weisz, D.R. Uncertain times: The redshift-time relation from cosmology and stars. *Mon. Not. R. Astron. Soc.* **2021**, *505*, 2764–2783. [CrossRef]
194. Vagnozzi, S.; Pacucci, F.; Loeb, A. Implications for the Hubble tension from the ages of the oldest astrophysical objects. *J. High Energy Astrophys.* **2022**, *36*, 27–35. [CrossRef]
195. Cimatti, A.; Moresco, M. Revisiting oldest stars as cosmological probes: New constraints on the Hubble constant. *arXiv* **2023**, arXiv:2302.07899.
196. Boylan-Kolchin, M. Stress testing ΛCDM with high-redshift galaxy candidates. *Nat. Astron.* **2023**, *7*, 731–735. [CrossRef]
197. Moresco, M.; Cimatti, A.; Jimenez, R.; Pozzetti, L.; Zamorani, G.; Bolzonella, M.; Dunlop, J.; Lamareille, F.; Mignoli, M.; Pearce, H.; et al. Improved constraints on the expansion rate of the Universe up to $z \sim 1.1$ from the spectroscopic evolution of cosmic chronometers. *J. Cosmol. Astropart. Phys.* **2012**, *2012*, 006. [CrossRef]
198. Holsclaw, T.; Alam, U.; Sansó, B.; Lee, H.; Heitmann, K.; Habib, S.; Higdon, D. Nonparametric reconstruction of the dark energy equation of state. *Phys. Rev. D* **2010**, *82*, 103502. [CrossRef]
199. Holsclaw, T.; Alam, U.; Sansó, B.; Lee, H.; Heitmann, K.; Habib, S.; Higdon, D. Nonparametric Dark Energy Reconstruction from Supernova Data. *Phys. Rev. Lett.* **2010**, *105*, 241302. [CrossRef]
200. Bargiacchi, G.; Risaliti, G.; Benetti, M.; Capozziello, S.; Lusso, E.; Saccardi, A.; Signorini, M. Cosmography by orthogonalized logarithmic polynomials. *Astron. Astrophys.* **2021**, *649*, A65. [CrossRef]
201. Amati, L.; Frontera, F.; Tavani, M.; in't Zand, J.J.M.; Antonelli, A.; Costa, E.; Feroci, M.; Guidorzi, C.; Heise, J.; Masetti, N.; et al. Intrinsic spectra and energetics of BeppoSAX Gamma-Ray Bursts with known redshifts. *Astron. Astrophys.* **2002**, *390*, 81–89. [CrossRef]
202. Ghirlanda, G.; Ghisellini, G.; Lazzati, D. The Collimation-corrected Gamma-Ray Burst Energies Correlate with the Peak Energy of Their νF_ν Spectrum. *Astrophys. J.* **2004**, *616*, 331–338. [CrossRef]
203. Dainotti, M.G.; Cardone, V.F.; Capozziello, S. A time-luminosity correlation for γ-ray bursts in the X-rays. *Mon. Not. R. Astron. Soc. Lett.* **2008**, *391*, L79–L83. [CrossRef]
204. Kumar, P.; Zhang, B. The physics of gamma-ray bursts and relativistic jets. *Phys. Rep.* **2015**, *561*, 1–109. [CrossRef]
205. Dainotti, M.G.; Lenart, A.L.; Sarracino, G.; Nagataki, S.; Capozziello, S.; Fraija, N. The X-ray Fundamental Plane of the Platinum Sample, the Kilonovae, and the SNe Ib/c Associated with GRBs. *Astrophys. J.* **2020**, *904*, 97. [CrossRef]
206. Cardone, V.F.; Capozziello, S.; Dainotti, M.G. An updated gamma-ray bursts Hubble diagram. *Mon. Not. R. Astron. Soc.* **2009**, *400*, 775–790. [CrossRef]
207. Cardone, V.F.; Dainotti, M.G.; Capozziello, S.; Willingale, R. Constraining cosmological parameters by gamma-ray burst X-ray afterglow light curves. *Mon. Not. R. Astron. Soc.* **2010**, *408*, 1181–1186. [CrossRef]
208. Amati, L.; D'Agostino, R.; Luongo, O.; Muccino, M.; Tantalo, M. Addressing the circularity problem in the Ep-Eiso correlation of gamma-ray bursts. *Mon. Not. R. Astron. Soc. Lett.* **2019**, *486*, L46–L51. [CrossRef]
209. Dainotti, M.G.; Lenart, A.L.; Chraya, A.; Sarracino, G.; Nagataki, S.; Fraija, N.; Capozziello, S.; Bogdan, M. The gamma-ray bursts fundamental plane correlation as a cosmological tool. *Mon. Not. R. Astron. Soc.* **2022**, *518*, 2201–2240. [CrossRef]
210. Bargiacchi, G.; Dainotti, M.G.; Nagataki, S.; Capozziello, S. Gamma-ray bursts, quasars, baryonic acoustic oscillations, and supernovae Ia: New statistical insights and cosmological constraints. *Mon. Not. R. Astron. Soc.* **2023**, *521*, 3909–3924. [CrossRef]
211. Dainotti, M.G.; Nielson, V.; Sarracino, G.; Rinaldi, E.; Nagataki, S.; Capozziello, S.; Gnedin, O.Y.; Bargiacchi, G. Optical and X-ray GRB Fundamental Planes as cosmological distance indicators. *Mon. Not. R. Astron. Soc.* **2022**, *514*, 1828–1856. [CrossRef]
212. Risaliti, G.; Lusso, E. A hubble diagram for quasars. *Astrophys. J.* **2015**, *815*, 33. [CrossRef]
213. Risaliti, G.; Lusso, E. Cosmological Constraints from the Hubble Diagram of Quasars at High Redshifts. *Nat. Astron.* **2019**, *3*, 272–277. [CrossRef]
214. Bargiacchi, G.; Benetti, M.; Capozziello, S.; Lusso, E.; Risaliti, G.; Signorini, M. Quasar cosmology: Dark energy evolution and spatial curvature. *Mon. Not. R. Astron. Soc.* **2022**, *515*, 1795–1806. [CrossRef]

215. Lenart, A.L.; Bargiacchi, G.; Dainotti, M.G.; Nagataki, S.; Capozziello, S. A Bias-free Cosmological Analysis with Quasars Alleviating H_0 Tension. *Astrophys. J. Suppl. Ser.* **2023**, *264*, 46. [CrossRef]
216. Risaliti, G.; Lusso, E.; Nardini, E.; Bargiacchi, G.; Bisogni, S.; Sacchi, A.; Signorini, M.; Trefoloni, B. Quasars as high-redshift standard candles. *Astron. Nachrichten* **2023**, *344*, e230054. [CrossRef]
217. Signorini, M.; Risaliti, G.; Lusso, E.; Nardini, E.; Bargiacchi, G.; Sacchi, A.; Trefoloni, B. Quasars as standard candles. *Astron. Astrophys.* **2023**, *676*, A143. [CrossRef]
218. Dainotti, M.G.; Bargiacchi, G.; Lenart, A.Ł.; Nagataki, S.; Capozziello, S. Quasars: Standard Candles up to z = 7.5 with the Precision of Supernovae Ia. *Astrophys. J.* **2023**, *950*, 45. [CrossRef]
219. Psaltis, D. Probes and Tests of Strong-Field Gravity with Observations in the Electromagnetic Spectrum. *Living Rev. Relativ.* **2008**, *11*, 9. [CrossRef]
220. Feola, P.; Forteza, X.J.; Capozziello, S.; Cianci, R.; Vignolo, S. Mass-radius relation for neutron stars in $f(R) = R + \alpha R^2$ gravity: A comparison between purely metric and torsion formulations. *Phys. Rev. D* **2020**, *101*, 044037. [CrossRef]
221. Peebles, P.J.E.; Ratra, B. Cosmology with a Time-Variable Cosmological "Constant". *Astrophys. J. Lett.* **1988**, *325*, L17. [CrossRef]
222. Ratra, B.; Peebles, P.J.E. Cosmological consequences of a rolling homogeneous scalar field. *Phys. Rev. D* **1988**, *37*, 3406–3427. [CrossRef]
223. Copeland, E.J.; Sami, M.; Tsujikawa, S. Dynamics Of Dark Energy. *Int. J. Mod. Phys. D* **2006**, *15*, 1753–1935. [CrossRef]
224. Chevallier, M.; Polarski, D. Accelerating Universes with Scaling Dark Matter. *Int. J. Mod. Phys. D* **2001**, *10*, 213–223. [CrossRef]
225. Linder, E.V. Exploring the Expansion History of the Universe. *Phys. Rev. Lett.* **2003**, *90*, 091301. [CrossRef]
226. Piedipalumbo, E.; Scudellaro, P.; Esposito, G.; Rubano, C. A matter-dominated cosmological model with variable G and Λ and its confrontation with observational data. *Gen. Relativ. Gravit.* **2012**, *44*, 2477–2501. [CrossRef]
227. Bonometto, S.; Mezzetti, M.; Mainini, R. Strongly coupled dark energy with warm dark matter vs. LCDM. *J. Cosmol. Astropart. Phys.* **2017**, *2017*, 011. [CrossRef]
228. Valentino, E.D.; Mena, O.; Pan, S.; Visinelli, L.; Yang, W.; Melchiorri, A.; Mota, D.F.; Riess, A.G.; Silk, J. In the realm of the Hubble tension-a review of solutions. *Class. Quantum Gravity* **2021**, *38*, 153001. [CrossRef]
229. Perivolaropoulos, L.; Skara, F. Challenges for ΛCDM: An update. *New Astron. Rev.* **2022**, *95*, 101659. [CrossRef]
230. Schöneberg, N.; Abellán, G.F.; Sánchez, A.P.; Witte, S.J.; Poulin, V.; Lesgourgues, J. The H_0 Olympics: A fair ranking of proposed models. *Phys. Rep.* **2022**, *984*, 1–55. [CrossRef]
231. Karwal, T.; Kamionkowski, M. Dark energy at early times, the Hubble parameter, and the string axiverse. *Phys. Rev. D* **2016**, *94*, 103523. [CrossRef]
232. Hill, J.C.; McDonough, E.; Toomey, M.W.; Alexander, S. Early dark energy does not restore cosmological concordance. *Phys. Rev. D* **2020**, *102*, 043507. [CrossRef]
233. Niedermann, F.; Sloth, M.S. New early dark energy is compatible with current LSS data. *Phys. Rev. D* **2021**, *103*, 103537. [CrossRef]
234. Mangano, G.; Miele, G.; Pastor, S.; Pinto, T.; Pisanti, O.; Serpico, P.D. Relic neutrino decoupling including flavour oscillations. *Nucl. Phys. B* **2005**, *729*, 221–234. [CrossRef]
235. Jacques, T.D.; Krauss, L.M.; Lunardini, C. Additional light sterile neutrinos and cosmology. *Phys. Rev. D* **2013**, *87*, 083515. [CrossRef]
236. Weinberg, S. Goldstone Bosons as Fractional Cosmic Neutrinos. *Phys. Rev. Lett.* **2013**, *110*, 241301. [CrossRef]
237. Allahverdi, R.; Cicoli, M.; Dutta, B.; Sinha, K. Correlation between dark matter and dark radiation in string compactifications. *J. Cosmol. Astropart. Phys.* **2014**, *2014*, 002. [CrossRef]
238. Valentino, E.D.; Giusarma, E.; Mena, O.; Melchiorri, A.; Silk, J. Cosmological limits on neutrino unknowns versus low redshift priors. *Phys. Rev. D* **2016**, *93*, 083527. [CrossRef]
239. Hart, L.; Chluba, J. New constraints on time-dependent variations of fundamental constants using Planck data. *Mon. Not. R. Astron. Soc.* **2017**, *474*, 1850–1861. [CrossRef]
240. Jedamzik, K.; Pogosian, L. Relieving the Hubble Tension with Primordial Magnetic Fields. *Phys. Rev. Lett.* **2020**, *125*, 181302. [CrossRef]
241. Bose, B.; Lombriser, L. Easing cosmic tensions with an open and hotter universe. *Phys. Rev. D* **2021**, *103*, L081304. [CrossRef]
242. Brevik, I.; Gorbunova, O. Dark energy and viscous cosmology. *Gen. Relativ. Gravit.* **2005**, *37*, 2039–2045. [CrossRef]
243. Wang, D.; Yan, Y.J.; Meng, X.H. A new pressure-parametrization unified dark fluid model. *Eur. Phys. J. C* **2017**, *77*, 263. [CrossRef]
244. Yang, W.; Pan, S.; Valentino, E.D.; Paliathanasis, A.; Lu, J. Challenging bulk viscous unified scenarios with cosmological observations. *Phys. Rev. D* **2019**, *100*, 103518. [CrossRef]
245. da Silva, W.J.C.; Silva, R. Growth of matter perturbations in the extended viscous dark energy models. *Eur. Phys. J. C* **2021**, *81*, 403. [CrossRef]
246. Khoury, J.; Weltman, A. Chameleon Fields: Awaiting Surprises for Tests of Gravity in Space. *Phys. Rev. Lett.* **2004**, *93*, 171104. [CrossRef] [PubMed]
247. Khoury, J.; Weltman, A. Chameleon cosmology. *Phys. Rev. D* **2004**, *69*, 044026. [CrossRef]
248. Vagnozzi, S.; Visinelli, L.; Brax, P.; Davis, A.C.; Sakstein, J. Direct detection of dark energy: The XENON1T excess and future prospects. *Phys. Rev. D* **2021**, *104*, 063023. [CrossRef]

249. Cai, R.G.; Guo, Z.K.; Li, L.; Wang, S.J.; Yu, W.W. Chameleon dark energy can resolve the Hubble tension. *Phys. Rev. D* **2021**, *103*, L121302. [CrossRef]
250. Benisty, D.; Davis, A.C. Dark energy interactions near the Galactic Center. *Phys. Rev. D* **2022**, *105*, 024052. [CrossRef]
251. Haba, Z.; Stachowski, A.; Szydłowski, M. Dynamics of the diffusive DM-DE interaction–Dynamical system approach. *J. Cosmol. Astropart. Phys.* **2016**, *2016*, 024. [CrossRef]
252. Koutsoumbas, G.; Ntrekis, K.; Papantonopoulos, E.; Saridakis, E.N. Unification of dark matter-dark energy in generalized Galileon theories. *J. Cosmol. Astropart. Phys.* **2018**, *2018*, 003. [CrossRef]
253. Calogero, S.; Velten, H. Cosmology with matter diffusion. *J. Cosmol. Astropart. Phys.* **2013**, *2013*, 025. [CrossRef]
254. Perez, A.; Sudarsky, D.; Wilson-Ewing, E. Resolving the H_0 tension with diffusion. *Gen. Relativ. Gravit.* **2021**, *53*, 7. [CrossRef]
255. Li, X.; Shafieloo, A. A Simple Phenomenological Emergent Dark Energy Model can Resolve the Hubble Tension. *Astrophys. J.* **2019**, *883*, L3. [CrossRef]
256. Pan, S.; Yang, W.; Valentino, E.D.; Shafieloo, A.; Chakraborty, S. Reconciling H_0 tension in a six parameter space? *J. Cosmol. Astropart. Phys.* **2020**, *2020*, 062. [CrossRef]
257. Rezaei, M.; Naderi, T.; Malekjani, M.; Mehrabi, A. A Bayesian comparison between ΛCDM and phenomenologically emergent dark energy models. *Eur. Phys. J. C* **2020**, *80*, 374. [CrossRef]
258. Solà , J. Cosmological constant and vacuum energy: Old and new ideas. *J. Phys. Conf. Ser.* **2013**, *453*, 012015. [CrossRef]
259. Solà , J.; Gómez-Valent, A. The $\bar{\Lambda}CDM$ cosmology: From inflation to dark energy through running Λ. *Int. J. Mod. Phys. D* **2015**, *24*, 1541003. [CrossRef]
260. Peracaula, J.S.; de Cruz Pérez, J.; Gómez-Valent, A. Possible signals of vacuum dynamics in the Universe. *Mon. Not. R. Astron. Soc.* **2018**, *478*, 4357–4373. [CrossRef]
261. Gómez-Valent, A.; Peracaula, J.S. Density perturbations for running vacuum: A successful approach to structure formation and to the σ8-tension. *Mon. Not. R. Astron. Soc.* **2018**, *478*, 126–145. [CrossRef]
262. Camarena, D.; Marra, V. Impact of the cosmic variance on H_0 on cosmological analyses. *Phys. Rev. D* **2018**, *98*, 023537. [CrossRef]
263. Bengaly, C.A.P.; Andrade, U.; Alcaniz, J.S. How does an incomplete sky coverage affect the Hubble Constant variance? *Eur. Phys. J. C* **2019**, *79*, 768. [CrossRef]
264. Krishnan, C.; Mohayaee, R.; Colgáin, E.O.; Sheikh-Jabbari, M.; Yin, L. Hints of FLRW breakdown from supernovae. *Phys. Rev. D* **2022**, *105*, 063514. [CrossRef]
265. Kalbouneh, B.; Marinoni, C.; Bel, J. Multipole expansion of the local expansion rate. *Phys. Rev. D* **2023**, *107*, 023507. [CrossRef]
266. Giani, L.; Howlett, C.; Said, K.; Davis, T.; Vagnozzi, S. An effective description of Laniakea: Impact on cosmology and the local determination of the Hubble constant. *J. Cosmol. Astropart. Phys.* **2024**, *2024*, 071. [CrossRef]
267. Helayël-Neto, J.A.; Spallicci, A.D.A.M. Frequency variation for *Vacuo* Photon Propag. Standard-Model Extension. *Eur. Phys. J. C* **2019**, *79*, 590. [CrossRef]
268. Bonetti, L.; dos Santos Filho, L.R.; Helayël-Neto, J.A.; Spallicci, A.D.A.M. Effective photon mass from Super and Lorentz symmetry breaking. *Phys. Lett. B* **2017**, *764*, 203. [CrossRef]
269. Bonetti, L.; dos Santos Filho, L.R.; Helayël-Neto, J.A.; Spallicci, A.D.A.M. Photon sector analysis of Super and Lorentz symmetry breaking: effective photon mass, bi-refringence and dissipation. *Eur. Phys. J. C* **2018**, *78*, 811. [CrossRef]
270. Goldhaber, A.S.; Nieto, M.M. Photon and graviton mass limits. *Rev. Mod. Phys.* **2010**, *82*, 939. [CrossRef]
271. Retinò, A.; Spallicci, A.D.A.M.; Vaivads, A. Solar wind test of the de Broglie-Proca massive photon with Cluster multi-spacecraft data. *Astropart. Phys.* **2016**, *82*, 49. [CrossRef]
272. de Broglie, L. *Nouvelles Recherches sur la Lumière*; Actualités Scientifiques et Industrielles; Hermann & Cie: Paris, France, 1936; Volume 411.
273. Proca, A. Sur les équations fondamentales des particules élémentaires. *C. R. Acad. Sci. Paris* **1936**, *202*, 1490.
274. Kumar Aluri, P.; Cea, P.; Chingangbam, P.; Chu, M.C.; Clowes, R.G.; Hutsemékers, D.; Kochappan, J.P.; Lopez, A.M.; Liu, L.; Martens, N.C.M.; et al. Is the observable Universe consistent with the cosmological principle? *Class. Quantum Gravity* **2023**, *40*, 094001. [CrossRef]
275. Krishnan, C.; Mondol, R.; Sheikh-Jabbari, M. Dipole cosmology: The Copernican paradigm beyond FLRW. *J. Cosmol. Astropart. Phys.* **2023**, *2023*, 020. [CrossRef]
276. Huang, C.D.; Riess, A.G.; Yuan, W.; Macri, L.M.; Zakamska, N.L.; Casertano, S.; Whitelock, P.A.; Hoffmann, S.L.; Filippenko, A.V.; Scolnic, D. Hubble Space Telescope Observations of Mira Variables in the SN Ia Host NGC 1559: An Alternative Candle to Measure the Hubble Constant. *Astrophys. J.* **2020**, *889*, 5. [CrossRef]
277. Farren, G.S.; Philcox, O.H.E.; Sherwin, B.D. Determining the Hubble constant without the sound horizon: Perspectives with future galaxy surveys. *Phys. Rev. D* **2022**, *105*, 063503. [CrossRef]
278. Yang, W.; Pan, S.; Vagnozzi, S.; Valentino, E.D.; Mota, D.F.; Capozziello, S. Dawn of the dark: Unified dark sectors and the EDGES Cosmic Dawn 21-cm signal. *J. Cosmol. Astropart. Phys.* **2019**, *2019*, 044. [CrossRef]
279. Bernardis, F.D.; Melchiorri, A.; Verde, L.; Jimenez, R. The cosmic neutrino background and the age of the Universe. *J. Cosmol. Astropart. Phys.* **2008**, *2008*, 020. [CrossRef]
280. Vandenberg, D.A.; Bolte, M.; Stetson, P.B. The Age of the Galactic Globular Cluster System. *Annu. Rev. Astron. Astrophys.* **1996**, *34*, 461–510. [CrossRef]
281. Soderblom, D.R. The Ages of Stars. *Annu. Rev. Astron. Astrophys.* **2010**, *48*, 581–629. [CrossRef]

282. Catelan, M. The ages of (the oldest) stars. *Proc. Int. Astron. Union* **2017**, *13*, 11–20. [CrossRef]
283. Valcin, D.; Bernal, J.L.; Jimenez, R.; Verde, L.; Wandelt, B.D. Inferring the age of the universe with globular clusters. *J. Cosmol. Astropart. Phys.* **2020**, *2020*, 002. [CrossRef]
284. Sazhin, M.V.; Sazhina, O.S.; Chadayammuri, U. The Scale Factor in the Universe with Dark Energy. *arXiv* **2011**, arXiv:astro-ph.CO/1109.2258.
285. Weinberg, E.J. Some problems with extended inflation. *Phys. Rev. D* **1989**, *40*, 3950–3959. [CrossRef]
286. Califano, M.; de Martino, I.; Vernieri, D.; Capozziello, S. Exploiting the Einstein Telescope to solve the Hubble tension. *Phys. Rev. D* **2023**, *107*, 123519. [CrossRef]
287. Califano, M.; de Martino, I.; Vernieri, D.; Capozziello, S. Constraining ΛCDM cosmological parameters with Einstein Telescope mock data. *Mon. Not. R. Astron. Soc.* **2022**, *518*, 3372–3385. [CrossRef]
288. Laureijs, R.; Amiaux, J.; Arduini, S.; Auguères, J.L.; Brinchmann, J.; Cole, R.; Cropper, M.; Dabin, C.; Duvet, L.; Ealet, A.; et al. Euclid Definition Study Report. *arXiv* **2011**, arXiv:astro-ph.CO/1110.3193.
289. Scaramella, R.; Amiaux, J.; Mellier, Y.; Burigana, C.; Carvalho, C.S.; Cuillandre, J.C.; Silva, A.D.; Derosa, A.; Dinis, J.; Maiorano, E.; et al. Euclid preparation. I. The Euclid Wide Survey. *Astron. Astrophys.* **2022**, *662*, A112. [CrossRef]
290. Blanchard, A.; Camera, S.; Carbone, C.; Cardone, V.F.; Casas, S.; Clesse, S.; Ilić , S.; Kilbinger, M.; Kitching, T.; Kunz, M.; et al. Euclid preparation. VII. Forecast validation for Euclid cosmological probes. *Astron. Astrophys.* **2020**, *642*, A191. [CrossRef]
291. Frusciante, N.; Pace, F.; Cardone, V.F.; Casas, S.; Tutusaus, I.; Ballardini, M.; Bellini, E.; Benevento, G.; Bose, B.; Valageas, P.; et al. Euclid: Constraining linearly scale-independent modifications of gravity with the spectroscopic and photometric primary probes. *arXiv* **2023**, arXiv:astro-ph.CO/2306.12368.
292. Casas, S.; Cardone, V.F.; Sapone, D.; Frusciante, N.; Pace, F.; Parimbelli, G.; Archidiacono, M.; Koyama, K.; Tutusaus, I.; Camera, S.; et al. Euclid: Constraints on $f(R)$ cosmologies from the spectroscopic and photometric primary probes. *arXiv* **2023**, arXiv:astro-ph.CO/2306.11053.
293. Bailey, A.C.; Vincenzi, M.; Scolnic, D.; Cuillandre, J.C.; Rhodes, J.; Hook, I.; Peterson, E.R.; Popovic, B. Type Ia supernova observations combining data from the Euclid mission and the Vera C. Rubin Observatory. *Mon. Not. R. Astron. Soc.* **2023**, *524*, 5432–5441. [CrossRef]
294. Joudaki, S.; Blake, C.; Heymans, C.; Choi, A.; Harnois-Deraps, J.; Hildebrandt, H.; Joachimi, B.; Johnson, A.; Mead, A.; Parkinson, D.; et al. CFHTLenS revisited: Assessing concordance with Planck including astrophysical systematics. *Mon. Not. R. Astron. Soc.* **2016**, *465*, 2033–2052. [CrossRef]
295. Abbott, T.; Aguena, M.; Alarcon, A.; Allam, S.; Alves, O.; Amon, A.; Andrade-Oliveira, F.; Annis, J.; Avila, S.; Bacon, D.; et al. Dark Energy Survey Year 3 results: Cosmological constraints from galaxy clustering and weak lensing. *Phys. Rev. D* **2022**, *105*, 023520. [CrossRef]
296. Di Valentino, E.; Melchiorri, A.; Silk, J. Planck evidence for a closed Universe and a possible crisis for cosmology. *Nat. Astron.* **2019**, *4*, 196–203. [CrossRef]
297. Challinor, A. CMB anisotropy science: A review. *Proc. Int. Astron. Union* **2012**, *8*, 42–52. [CrossRef]
298. Schwarz, D.J.; Copi, C.J.; Huterer, D.; Starkman, G.D. CMB anomalies after Planck. *Class. Quantum Gravity* **2016**, *33*, 184001. [CrossRef]
299. Akrami, Y.; Ashdown, M.; Aumont, J.; Baccigalupi, C.; Ballardini, M.; Banday, A.J.; Barreiro, R.B.; Bartolo, N.; Basak, S.; Benabed, K.; et al. Planck2018 results: VII. Isotropy and statistics of the CMB. *Astron. Astrophys.* **2020**, *641*, A7. [CrossRef]

Disclaimer/Publisher's Note: The statements, opinions and data contained in all publications are solely those of the individual author(s) and contributor(s) and not of MDPI and/or the editor(s). MDPI and/or the editor(s) disclaim responsibility for any injury to people or property resulting from any ideas, methods, instructions or products referred to in the content.